SEMINAR

IX

Developments in the Design of Reinforced and Prestressed Concrete Structures

Développements dans le projet de constructions en béton armé et précontraint

Entwicklungen bei der Planung von Stahlbeton- und Spannbetonbauwerken

Chairman: J. Blaauwendraad, Netherlands

Coordinator: R. Favre, Switzerland

General Reporter: M. Wicke, Austria

The theme has been introduced by the General Reporter in the Introductory Report of the 12th Congress, available at the IABSE Secretariat.

Leere Seite

Blank page

Page vide

Reinforced Concrete Beams with High Tension Shear Reinforcement

Poutres en béton armé renforcées par des étriers à très haute résistance

Schubwiderstand von Stahlbetonbalken mit hochfestem Bewehrungsstahl

Masashi FUKUHARA
Research Associate
Tokyo Inst. of Tech.
Tokyo, Japan

Masashi Fukuhara, born 1936, graduated in Building Engineering from the Kogakuin Inst. of Technol. He is engaged in teaching and research in connection with aseismic problems in reinforced concrete structures.

Akira WADA
Assoc. Prof.
Tokyo Inst. of Tech.
Tokyo, Japan

Seiji KOKUSHO
Prof. Dr.
Tokyo Inst. of Tech.
Tokyo, Japan

SUMMARY
Reinforced concrete structures have frequently suffered heavy damage by shear failure in reinforced concrete members during strong earthquakes. This paper describes the experimental results concerning the effectiveness of the high tension shear reinforcement on the shear failure, and the analytical results concerning the shear transfer carried by the shear resistant elements across the critical inclined crack near the ultimate shear strength in beams.

RESUME
Des poutres en béton armé ont souvent souffert de grands dommages d'effort tranchant pendant les séismes. Cette contribution décrit les résultats expérimentaux concernant l'utilité d'étriers à très haute résistance et les résultats analytiques concernant le comportement de ces étriers avant la ruine.

ZUSAMMENFASSUNG
Bei starken Erdbeben wird bei Stahlbetonbauteilen oft Schubversagen beobachtet. Im Beitrag werden die experimentellen Ergebnisse über die Wirksamkeit hochfesten Bewehrungsstahls auf den Schubwiderstand vorgestellt und analytische Ergebnisse über die Schubkraftübertragung der Bewehrung im kritischen Riss präsentiert.

1. INTRODUCTION

Recent research works regarding the effectiveness of shear reinforcement have been primarily devoted to the members with the ordinary shear reinforcement whose yield stress was about 340 MPa. Although several investigations have included the members with the high tension shear reinforcement, the factors affecting the ultimate shear strength of members with the high tension shear reinforcement have not been systematically studied. Then, the experimental study was carried out in order to seize the real phenomenon concerning the effectiveness of the high tension shear reinforcement in beams. The analytical study was carried out in order to examine the mechanism of shear transfer carried by the shear resistant elements across the inclined crack near the ultimate shear strength. The analytical method was the FEM linear analysis using the models with some inclined cracks as many as the experimental results.

2. EXPERIMENRAL STUDY

2.1 Outline of the experimental study

Nine specimens designed to investigate the ultimate shear strength were tested as shown in Table 1. The primary factors were the shear span ratio a/D, the yield stress of the shear reinforcement $_w\sigma_y$ (MPa), and the shear reinforcement ratio p_w {%} as shown in Table 1. All specimens had the same cross section (b x D = 18cm x 40cm) as shown in Fig.1. The compressive strength $_c\sigma_B$ were 27.6 MPa in case of a/D =1.0, and the 31.8 MPa in case of a/D =1.5 , and the yield stress of or 0.2% proof stress of the shear reinforcement $_w\sigma_y$ were the range from 250 to 1370 MPa as shown in Table 1. The high tension shear reinforcement was the heat treated steel called ULUBON. Loading was carried out in an anti-symmetrical method as shown in Fig.2. The shear force P (N) was measured by the load cells between the oil jacks and the stubs of specimen, and the relative deformation δ(mm) was measured by the electric gages as shown in Fig.2.

No.	$_c\sigma_B$	a/D	p_w	$_w\sigma_y$	$_s\tau_c$	$_s\tau_u$	mode
1	27.6	1.0	0.0		1.10	1.87	S
2	27.6	1.0	0.34	345	1.82	4.87	S
3	27.6	1.0	0.34	1361	1.46	6.47	S
4	31.8	1.5	0.0		1.29	2.01	S
5	31.8	1.5	0.28	250	0.93	3.53	S
6	31.8	1.5	0.28	674	1.10	5.13	S
7	31.8	1.5	0.28	1322	0.96	6.04	S
8	31.8	1.5	0.56	250	1.27	4.58	S
9	31.8	1.5	0.56	1370	1.65	6.92	F

$_c\sigma_B$: Compressive strength of concrete (MPa)
a/D: Shear span ratio
p_w :Amount of shear reinforcement (%)
$_w\sigma_y$: Yield stress of shear reinforcement (MPa)
$_s\tau_c$: = Q_c/bj (MPa) Q_c: First inclined crack
$_s\tau_u$: = Q_u/bj (MPa) Q_u: Ultimate shear strength
S : Shear failure mode
F : Flexural failure mode

**Table 1** Specimens and Experimental Value
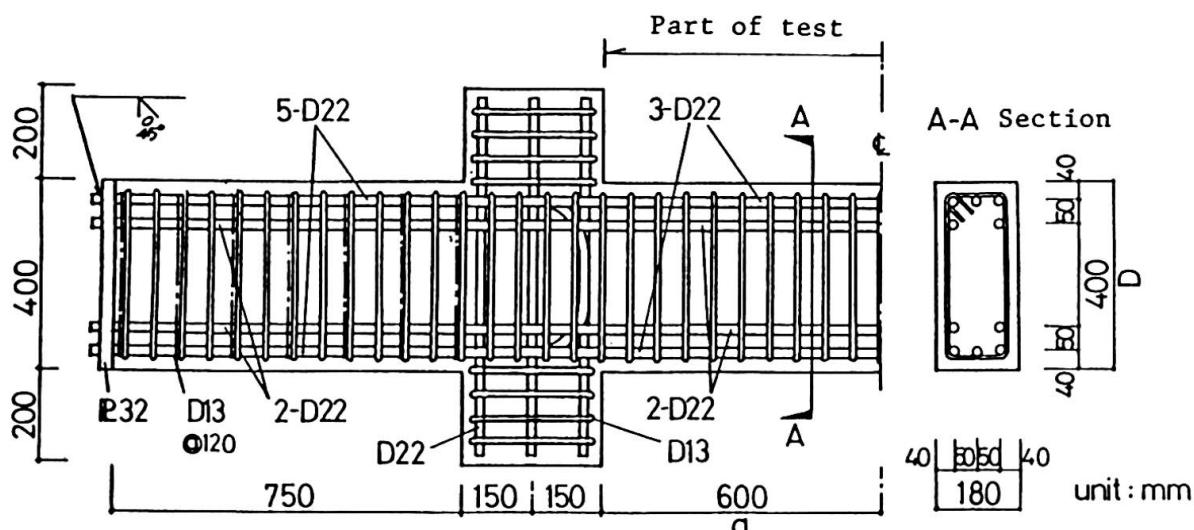
Fig.1 Specimen (a/D = 1.5)

2.2 Experimental results and discussion

2.2.1 Failure mode

The failure mode of specimens expect the No.9 was the shear failure type as shown in photo.1, and the failure mode of No.9 was the flexural failure type after the flexural tensile yielding of longitudinal reinforcement.

2.2.2 Effect of $_w\sigma_y$

Fig.3, 4 and 5 were the p(Mpa) - δ(mm) curves in case of a/D = 1.5 under the same value of p_w(= 0.28%) which the yield stress of shear reinforcement $_w\sigma_y$ in Fig.3, 4 and 5 was 354, 674 and 1323 Mpa.

The effectiveness of $_w\sigma_y$ on the shear strength and deformation capacity could be remarkably observed from those figures, so that it was found that the seismic ability of RC members colud be improved by using the high tension shear reinforcement instead of the ordinary strength.
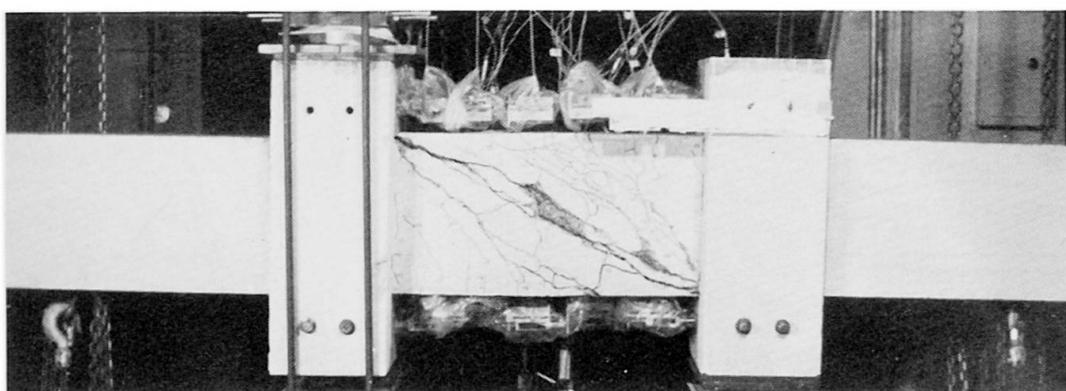
Photo.1 Behaviour of cracks after the shear failure (a/D=1.0)
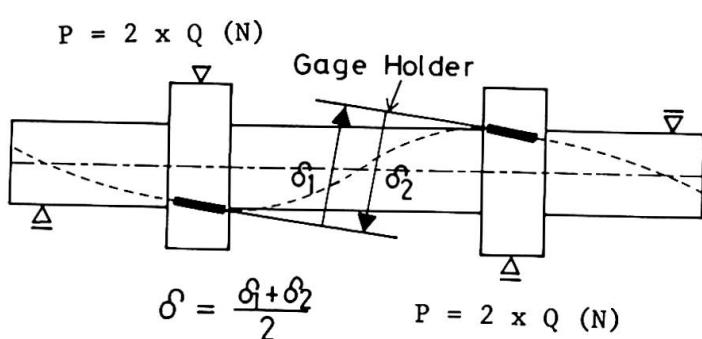

Fig.2 Loading and measuring method

$$\delta = \frac{\delta_1 + \delta_2}{2} \qquad P = 2 \times Q \ (N)$$
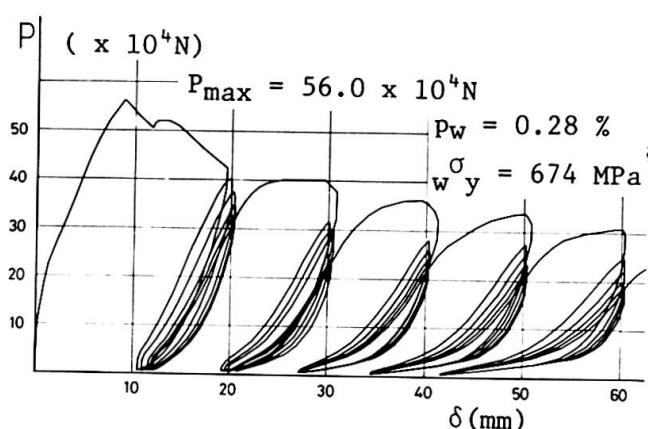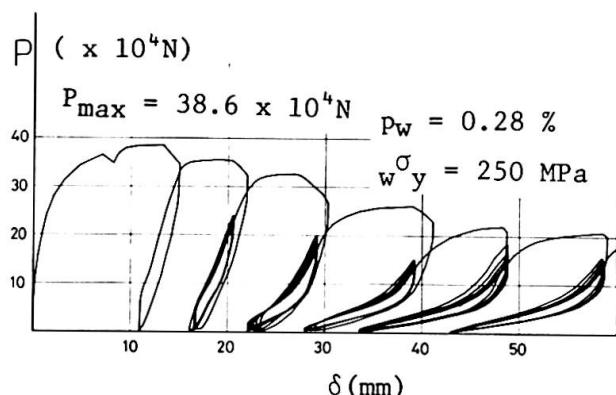

Fig.3 P − δcurve (No.5)

Fig.4 P − δ curve (No.6)
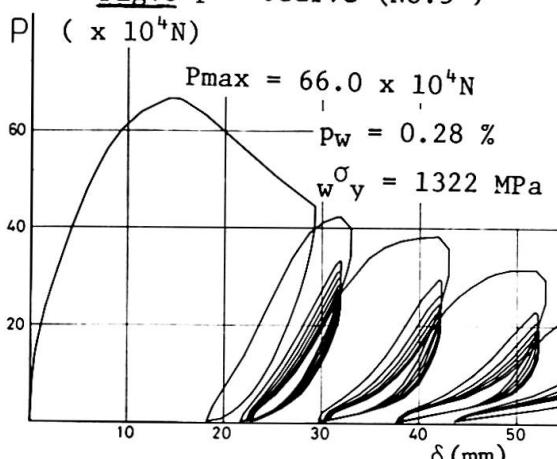
Fig.5 Q − δ curve (No.7)

2.2.3 Consideration for the effect of $_w\sigma_y$

Fig.6 and 7 show the P(Mpa) – δ(mm) curves under the same value of p_w(= 0.56%).
Fig.6 was with $_w\sigma_y$ =250 Mpa, and the Fig.7 was with $_w\sigma_y$ =1323 Mpa. As shown in
Fig.6 and 7, the effectiveness of high tension could be remarkably observed more
than ordinary strength too.
Fig.8 and 9 show the relation between the shear force and the strain of shear rein-
forcement measured by the wire strain gages in above specimens. Those figures
indicated the essential cause for the large effectiveness of the high tension shear
reinforcement on P(Mpa) – δ(mm) curves. After all, the strain of shear reinforce-
ment increased remarkably after the first inclined crack in both specimens. But as
soon as the ordinary shear reinforcement had reached near the yield strain (ε_y =
1214μ), the specimens with ordinary strength failured. On the other hand, the high
tension shear reinforcement not reached the yield strain (ε_y = 6424 μ) yet, so
that the specimen with the high tension could keep the more shear strength than the
specimen with ordinary strength.
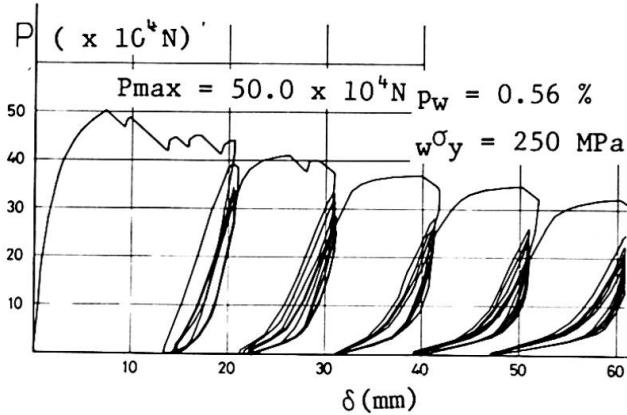


Fig.6 P – δ curve (No.8)
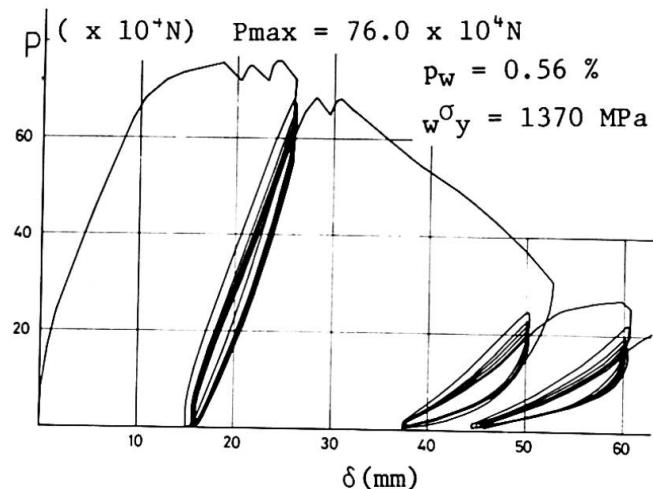

Fig.7 P – δ curve (No.9)
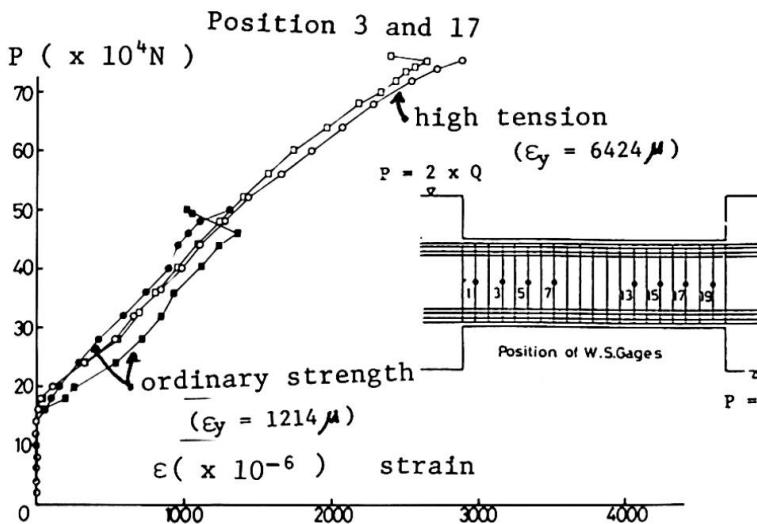
Fig.8 Relation between P and strain (3-17)
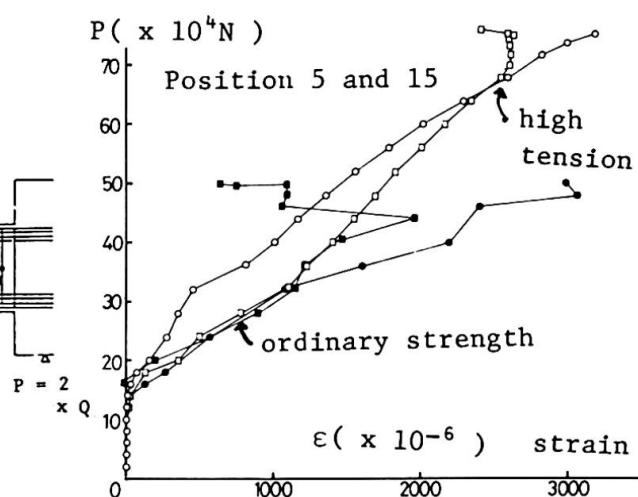
Fig.9 Relation between P and strain (5-

3. ANALYTICAL STUDY

3.1 Outline

The purpose in this analytical study is to investigate the shear transfer carried by the shear resistant elements across the critical inclined crack near ultimate shear strength. At first in this study, the analytical model having some inclined cracks as many as the experimental results on the shear failure was produced, and the reasonable propriety of the model was inspected. And then the shear transfer carried by the shear resistant elements across the inclined crack was examined by the results of the parameter analysis used this model subjected to the unit shear force Q_{unit} (= 98. $\times 10^2$ N = 1.0 tonf)

3.2 Analytical model

Fig.10 (a/D= 1.0) and 11 (a/D= 1.5) show the analytical models. FEM models was produced by refering to the shear behavior on the status that some inclined cracks occurred as shown in Photo.1. Fig.12 shows the relation between the shear force $_sQ_u$ and each shear transfer Q_w, Q_c, Q_d carried by the shear resistant elements across the inclined crack. The parameters in this model in case of a/D= 1.5 were the amount of the shear reinforcement ratio p_w(%), the yield stress of reinforcement $_w\sigma_y$ (Mpa) and the amount of the longitudinal reinforcement p_t, p_c(%). Elements properties (young's modulus E_c and E_s, poisson's ratio and bond links $_{x,y}K_b$) in this FEM model were used as shown in Table 2.
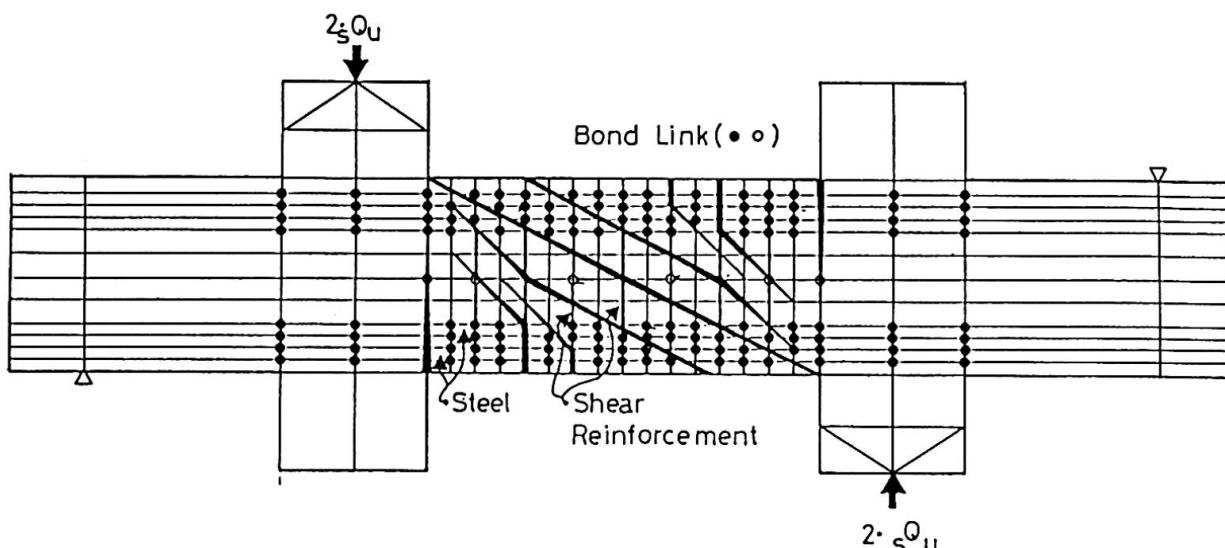
Fig.10 Analytical model (a/D = 1.0)
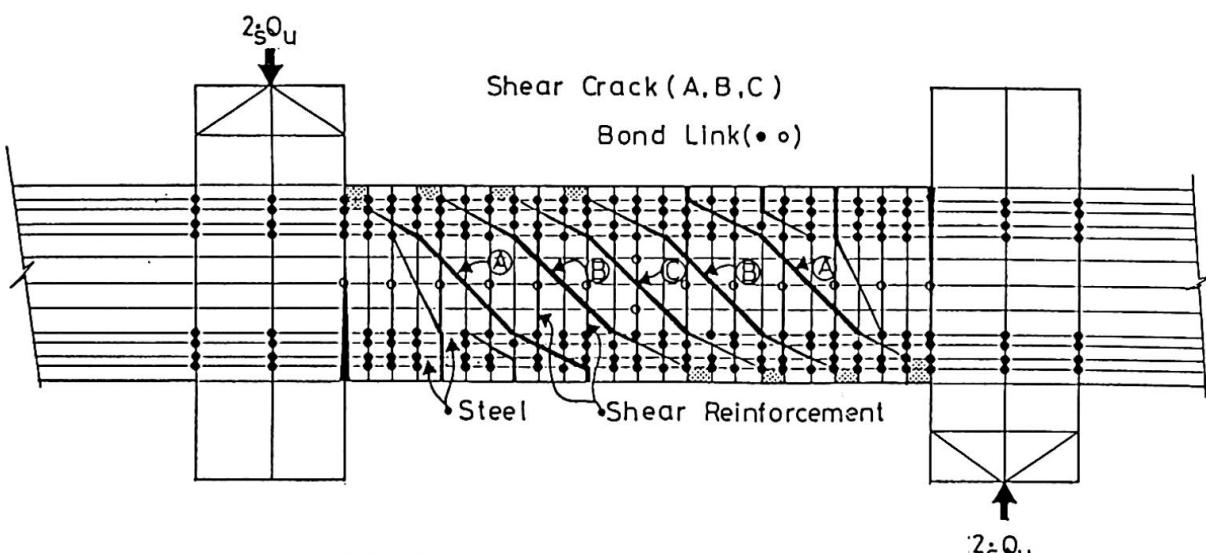
Fig.11 Analytical model (a/D = 1.5)

3.3 Discussion of analytical results

3.3.1 Analytical method

The comparison between the analytical and experimental results at the ultimate shear strength $_sQ_u$(=37.24 x 10^4N =38.0 tonf) were shown in following Fig.13. Fig.13 showed the strain distribution of shear reinforcement. It could be comfirmed that those analytical result nearly coincided with the experimental results in above figures, so that the analytical method was one of the effective methods in order to investigate the ultimate shear behavior in RC beams.

	Concrete element	Steel element
Young's modulus	2.0 x 10^4 MPa	2.0 x 10^5 MPa
Poisson's ratio	0.167	2.333
Bond link	$_xK_B = {}_yK_B = 2.0$ tonf/cm^3	

Table 2   Elements Properties
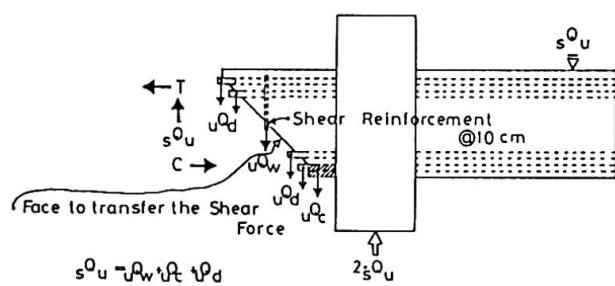
Fig.12 Equilibrium equation of shear force at inclined crack
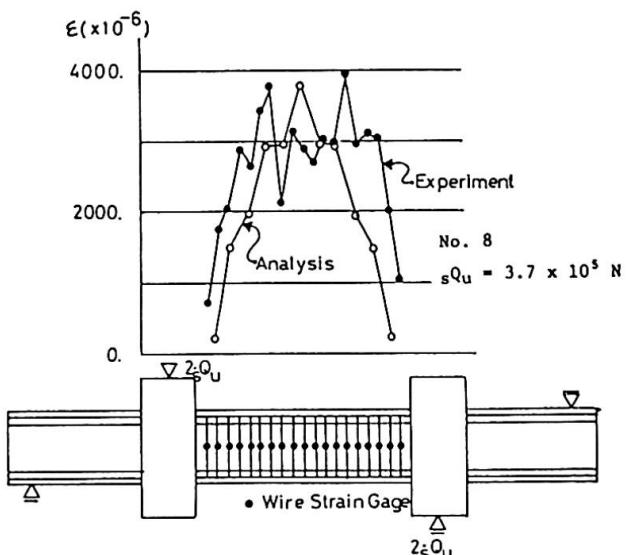
Fig.13 Strain distribution of shear reinforcemen

3.3.2 Effect of a/D

Fig.14 and 15 showed the distribution of compressive principal stress under the unit shear force Q_{unit}(= 98 x 10^2N = 1.0 tonf). Fig.14 was in case of a/D=1.0 and Fig.15 was in case of a/D=1.5. It was found that the compressive principal stress in a/D= 1.0 followed along the diagonal shear crack, on the other hand, that in a/D=1.5 dist-ributed amoung the whole of specimen as shown in Fig.14 and 15.
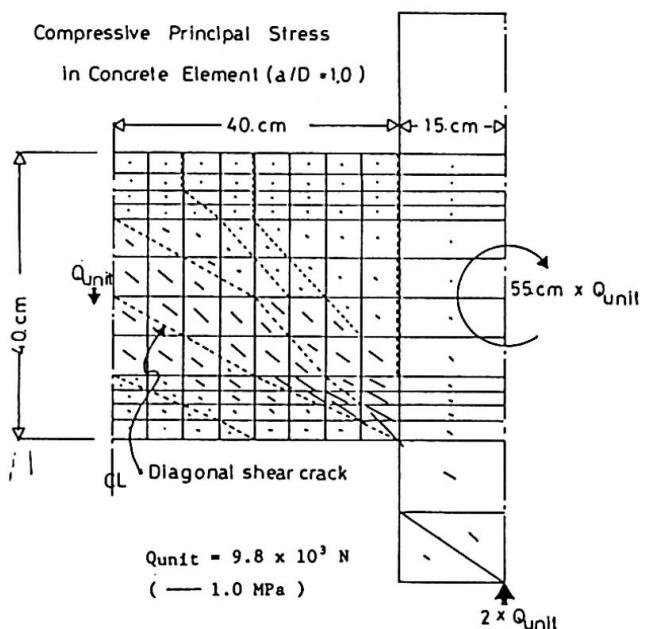
Fig.14 Compressive principal stress (a/D=1.0)
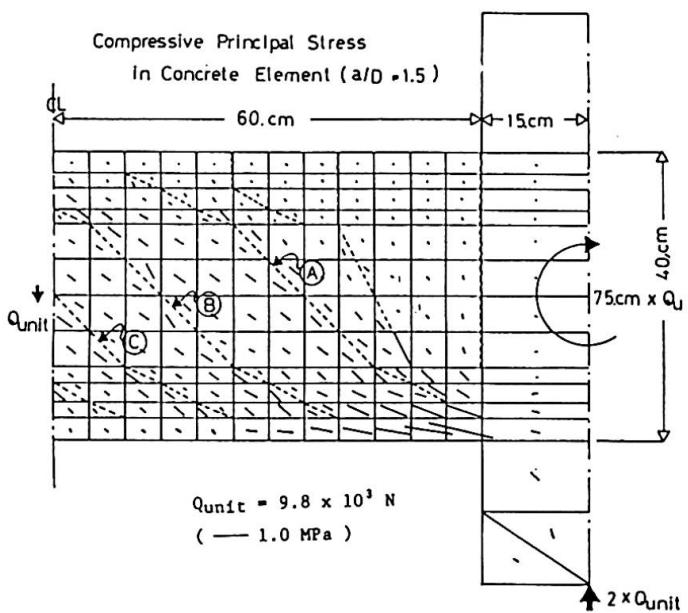
Fig.15 Compressive principal stress (a/D=1.5)
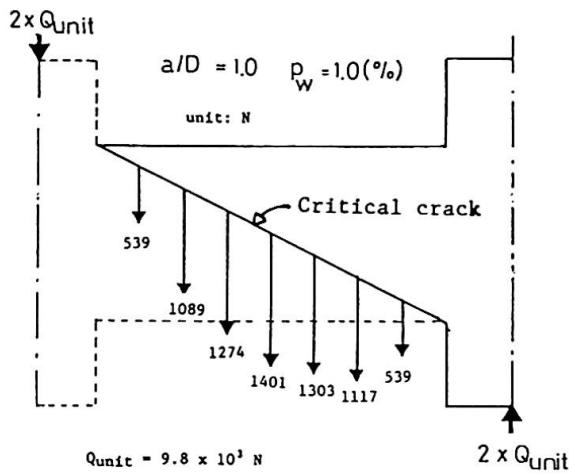
Fig 16 Shear stress of shear
       reinforcement (a/D = 1.0)
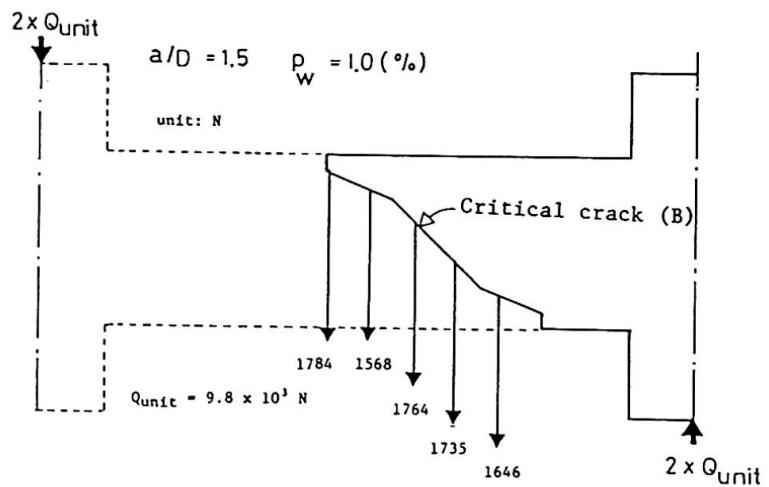
Fig.17 Shear stress of shear
       reinforcement (a/D=1.5)

3.3.3 Relation between p_W and $_WQ_{unit}$

Fig.18 shows the relation between $p_W(\%)$ and $_WQ_{unit}$. Here, $_WQ_{unit}$ is amount of the shear transfer carried by the shear reinforcement across the critical inclined crack. It was observed that the $_WQ_{unit}$ increased in propotion to p_W and the rate of increase on $_WQ_{unit}$ over about $p_W = 1.0\%$ came down as shown in Fig.18.

3.3.4 Relation between p_t, p_c and $_c\bar{\sigma}_{unit}$

Fig.19 shows the relation between p_t, $p_c(\%)$ and $_c\bar{\sigma}_{unit}$. Here, $p_t, p_c(\%)$ is the amount of longitudinal reinforcement and $_c\bar{\sigma}_{unit}$ is the average value of compressive stress appeared to the concrete element in compressive zone at the end of specimen as shown in Fig.19. It was clearly recognized that the shear behavior of concrete elements in compression zone was influenced by amount of the longitudinal reinforcement as shown in Fig.19.
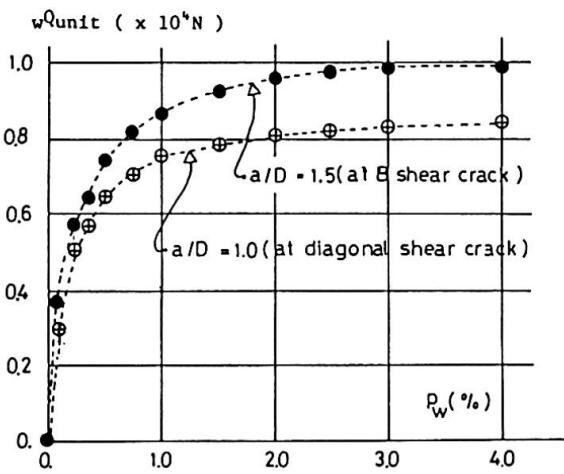
Fig.18 Relation between $_WQ_{unit}$ and p_W
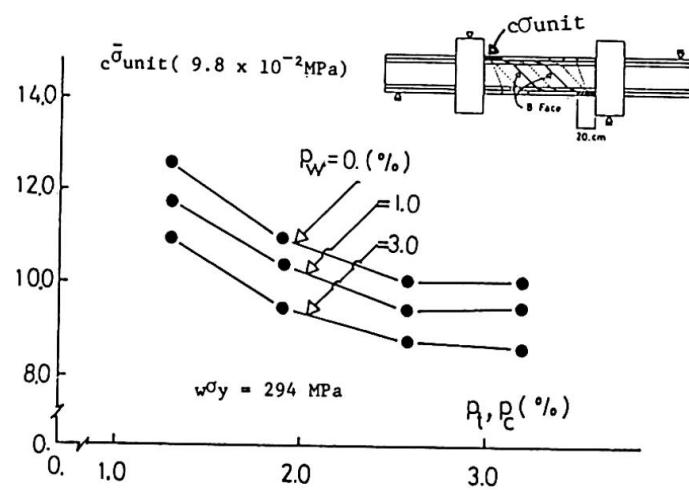
Fig.19 Relation between $_c\bar{\sigma}_{unit}$ and p_t, p_c

3.3.5 Relation between p_t, p_c and $_dQ_{unit}$

Fig.20 shows the relation between p_t, p_c(%) and $_dQ_{unit}$. Here, $_dQ_{unit}$ was the dowel shear carried by the longitudinal reinforcement across the critical inclined crack. It was observed that $_dQ_{unit}$ increased proportionally to p_t, p_c(%) and such tendency was indicated more remarkably in case of little p_w than in case of much p_w.
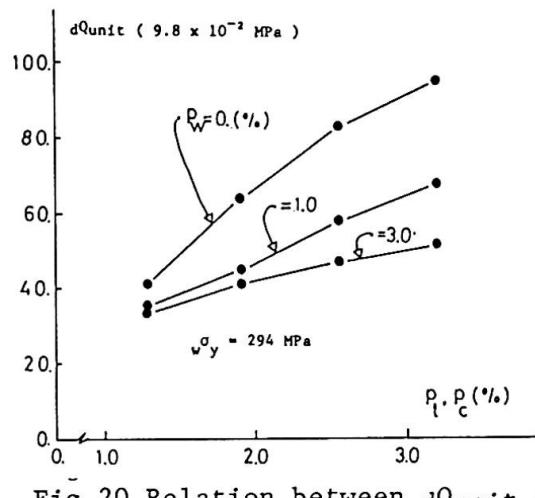
Fig.20 Relation between $_dQ_{unit}$ and p_t, p_c

4. CONCLUSIONS

Based on the experiment and analysis reported herein, the following conclusions can be drawn.

1) Effect of yield stress $(_w\sigma_y)$

It was found that the effect of $_w\sigma_y$ on the ultimate shear strength was remarkable in this experimental study, and the specimens with high tension shear reinforcement could possess more the ultimate shear strength than that with ordinary shear reinforcement for the same value of p_w(%).

2) Analytical model

It could be comfirmed that the FEM linear analysis using the analtyical model with some inclined cracks as many as experimental results was one of the effective method in order to investigate the shear transfer carried by the shear resistant elements across the critical inclined crack near the ultimate shear strength in reinforced concrete beams.

3) Shear transfer

The analytical results using the analytical model subjected to the unit shear force provided the information about the mechanism of the shear transfer carried by the shear resistant elements across the critical inclined crack.

Acknowledgement
The authors wish to thank NETUREN CO.,LTD. for their offering of the specimens.

REFERENCE
1.M.FUKUHARA,S.KOKUSHO.,Effectiveness of high tension shear reinforcement in reinforced concrete members, Trans. of A.I.J.Vol.320.oct.1980
2. M.FUKUHARA,S.KOKUSHO.,Shear trensfer carried by the shear reinforcement across the inclined crack near ultimate shear strength, Proc.of J.C.I.Vol.5.1983.
3. SCORDELIS.,Finite element analysis of reinforced concrete beams, Journal of A.C.I.Mar.1967
4. H.NOGUCHI., Shear resistance mechanism of reinforced concrete beams, Proc. of J.C.I Colloquim,1982.
5. A.H.MATTOCK,. Stirrup effectiveness in reinforced concrete beams with axial force, Journal of the structural division, sep.1971

New Design Concept for Reinforced Concrete Columns in Buildings

Approche nouvelle dans l'analyse des colonnes de bâtiment

Neues Bemessungsverfahren für Stahlbetonstützen in Gebäuden

R. FAVRE
Professor
Swiss Fed. Inst. Technol.
Lausanne, Switzerland

R. Favre worked in the consulting firm Schalcher & Favre before becoming Professor at the EPF Lausanne in 1973. His main research interests concern the service behaviour of concrete structures.

D. NAJDANOVIC
Research Assistant
Univ. of Belgrade
Belgrade, Yugoslavia

D. Najdanovic graduated at Belgrade Univ. in 1967 and is currently working on a PhD degree, a joint-venture project between the University of Belgrade and the EPF Lausanne.

R. SUTER
Scientific Adviser
Swiss Fed. Inst. Technol.
Lausanne, Switzerland

R. Suter joined the EPF Lausanne in 1969. He obtained in 1980 his PhD in structural engineering and has been scientific adviser since 1984.

C. THÜRLIMANN
Research Assistant
Swiss Fed. Inst. Technol.
Lausanne, Switzerland

C. Thürlimann worked for Freemann Fox & Partners, Consult. Eng., London after graduation in 1977. He has been at the EPF Lausanne since autumn 1979 where he obtained his PhD in 1984.

SUMMARY
Buildings are very often horizontally stabilized by means of a core or by shear walls. The columns in these buildings serve primarily to transfer the vertical loads. The columns are nevertheless subjected to imposed end deformations. A new design concept for reinforced concrete columns is proposed based on theoretical and experimental studies.

RESUME
Comme les colonnes de bâtiments sont avantageusement stabilisées dans le sens horizontal par des noyaux ou refends, ils ne servent qu'à reprendre les charges verticales tout en subissant des déformations imposées à leurs extrémités. A partir d'études théoriques et expérimentales, un nouveau concept de dimensionnement des colonnes est présenté.

ZUSAMMENFASSUNG
Da Gebäudestützen mit Vorteil durch Kerne oder Wände horizontal ausgesteift werden, dienen sie nur zur Übertragung der vertikalen Lasten, wobei ihnen an den Enden Verformungen aufgezwungen werden. Von theoretischen und experimentellen Untersuchungen ausgehend, wird ein neues Konzept für den Entwurf von Stützen dargestellt.

1. REASONS FOR A NEW CONCEPT

Two completely different attitudes can be observed in practice when civil engineers design reinforced concrete columns for buildings:

a) considering only the normal force, which considerably simplifies the problem,

b) regarding the flexural moment and the normal force, which leads to a frame analysation, sometimes considering the influence of the second order effects.

The first attitude leads often to a very good design provided that the engineer has sufficient design experience and feeling for design. The second attitude is one of the conscientious engineer who belives the correct solution can only result from complicated calculations.

Columns in buildings are a good example where the gain in knowledge which has been established over the last 20 years in the desing of reinforced concrete structures could be put into practice.

Theoretical studies and tests, based on the theory of plasticity, have proven the high ductility of reinforced concrete members, despite a certain reluctance to accept this theory, which is diminishing each year.

Moreover, the service behaviour of reinforced concrete members under compression has shown to be more favourable in reality what the crack problem concerns than predicted. Hence there is a need to adopte column design to current knowledge of column behaviour.

The high ductility of the columns often allows the complete suppression of expansion joints or large spacings. Due to the presence of cores, staircases or elevator cages, a multistorey building with columns can be conceived in the following manner (Fig. 1):

- spacing between the expansion joints between every 50 to 100 m,
- core and/or shear walls in reinforced concrete to take the horizontal loads,
- columns with a high degree of reinforcement ($\rho = 1$ to 15%) to take the vertical loads.

In conceiving a building in this way, it is necessary to consider the behaviour of the columns under imposed deformations. The columns follow deformations which are imposed on them by the bending or contracting of the floor slabs (Fig. 2).

It is not useful to calculate the moments in the frame joints. The calculation is made uncertain due to various effects such as crack formation in the slabs, the effective width of the slab and the adopted live load pattern etc.. It is preferable to verify that the columns have a sufficient axial load capacity to take the normal force and that they are ductile enough to withstand the imposed end deformations. It is evident that this ductility is higher the more slender the column is.
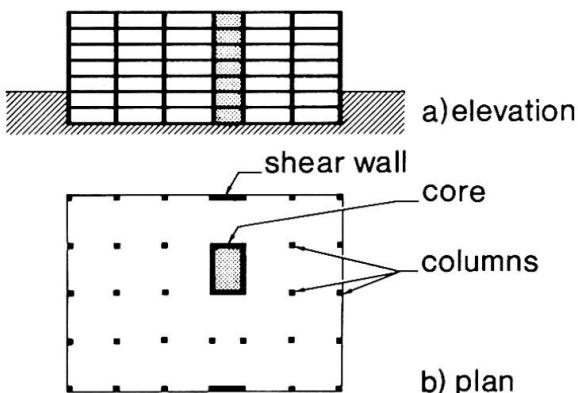

Fig. 1 Building with Core and
Shear Walls
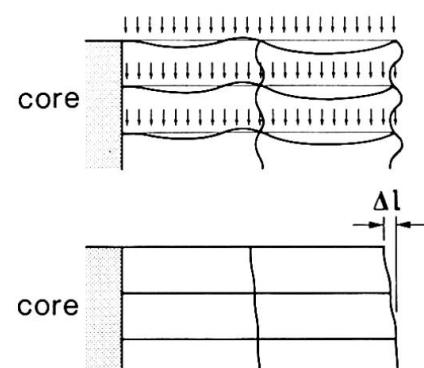
Fig. 2 Imposed Deformations on
Building

This may be achieved by choosing a high degree of reinforcement which allows a reduction of the dimensions of the columns leading to an economy of material.

2. DESIGN CRITERIA

The proposed column design method is based on limit state considerations.
The ultimate and the serviceability limit states of a column are verified by comparing the estimated imposed angles at the column end with the respective limit angles. The latter depend on the level of the applied normal force. Four different deformation cases can principally be distinguished (see Fig.3).
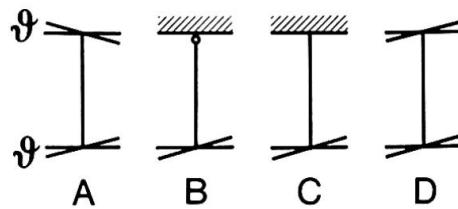
Fig. 3 Deformation Cases

2.1 Ultimate Limit State

Braced columns with a moderate slenderness ratio do not fail when their maximum flexural resistance is reached. They simply start to develop plastic hindges, which allow further large deformations to occur. The normal force starts to centre itself at the rotated column end after the maximum flexural resistance has been reached. The column fails when the deflection within the plastic hinge produces a moment which becomes equal to the remaining resistance. The imposed end deformations and the applied normal force are important for the design of a column and not the maximum flexural resistance.

Reinforced concrete columns with closely spaced stirrups show ductile behaviour under imposed deformations. Fig. 4 shows schematically the moment-curvature relationship of a column with a constant normal force.
The strains on the compression face are around 0.4 to 0.5 % when the column reaches the maximum flexural resistance. The concrete cover starts then to spall on the compression face.
Tests [1] show that strains of 2 % and more can be reached in the core if
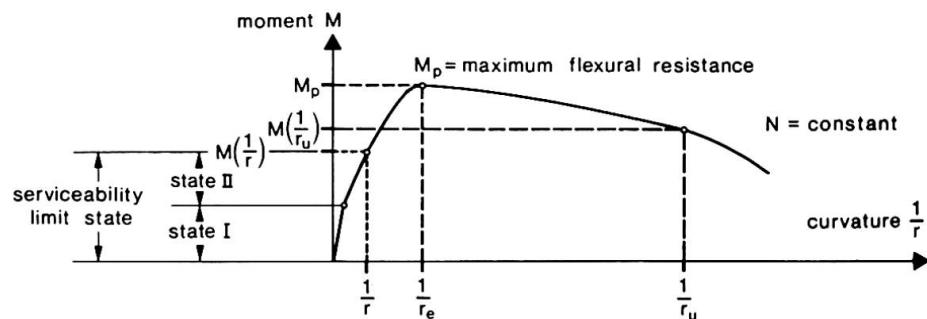
Fig. 4 Normal Force-Moment-Curvature Relationship :
Admissible $(1/r)$, Plastic $(1/r_e)$ and
Ultimate $(1/r_u)$ Limit Curvatures

	A	B	C	D
$\xi_e =$	$\dfrac{1}{4}\cdot\dfrac{1}{h}$	$\dfrac{1}{3}\cdot\dfrac{1}{h}$	$\dfrac{1}{4}\cdot\dfrac{1}{h}$	$\dfrac{1}{6}\cdot\dfrac{1}{h}$
$\xi_p =$	$\dfrac{1}{2}\cdot\lambda_p$	$\left(1-\dfrac{1}{2}\cdot\dfrac{h}{l}\cdot\lambda_p\right)\cdot\lambda_p$	$\left(1-\dfrac{3}{4}\cdot\dfrac{h}{l}\cdot\lambda_p\right)\cdot\lambda_p$	$\left(1-\dfrac{h}{l}\cdot\lambda_p\right)\cdot\lambda_p$
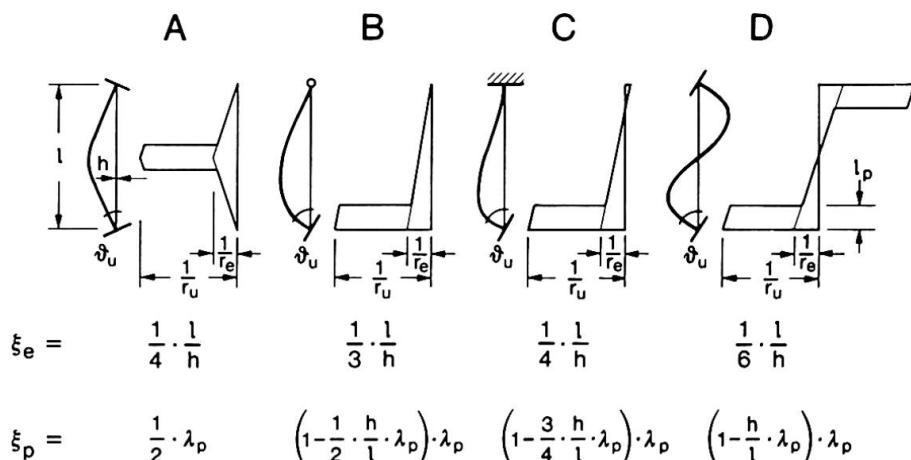
Fig. 5 Ultimate Limit Angle : Curvature Diagrams
and Coefficients ξ_e, ξ_p

the concrete is adequately confined by stirrups. An ultimate limit curvature can be fixed to $h/r_u = 10 \cdot \varepsilon_{yk}/\psi = 0.02/\psi$ (see [2]), with ψ equal to the ratio of the distance between the longitudinal reinforcement of opposite faces and the column width, h (see Fig. 14). A column with closely spaced stirrups (e.g. 50 mm) in the zone where the plastic hinge will occur can reach this curvature without buckling of the longitudinal bars and without any significant loss of resistance in the core concrete. The strains in the reinforcement bars on the compression face lie between 0 and 2% (10 times the yield strain of steel ε_{yk}) for that curvature, depending on the applied normal force.

A column with a very small or no normal force may reach larger curvatures in a plastic hinge as there is no danger of buckling of the reinforcement bars. The proposed limit is nevertheless considered to be sufficiently large to allow large plastic rotations. h/r_u equal the rotation of the plastic hinge if one assumes the length of the plastic hinge to be equal to the column width h and also if one assumes a constant curvature in the plastic hinge. For example with $\psi = 0.8$, the rotation of the plastic hinge is equal to 0.025 rad.

Fig. 5 shows the assumed curvature distribution for the columns which have reached the ultimate limit curvatures in the plastic hinge.

The elastic curvature distribution of deformation case A (Fig. 5) has been assumed to be triangular in order not to overestimate the ultimate limit angle as the maximum flexural resistance is reached at midspan. The ultimate limit angle is equal to

$$\vartheta_u = \xi_e \cdot h/r_e + \xi_p \cdot (h/r_u - h/r_e) \tag{1}$$

Design charts give the values for the curvatures h/r_e as a function of the applied normal force.

The value λ_p in coefficient ξ_p is defined as $\lambda_p = \ell_p/h$ with ℓ_p equal to the length of the plastic hinge. $\ell_p = 0.5 \cdot h$, h or $2 \cdot h$ respectively can be used in the estimation of the ultimate limit angle provided that the column has closely spaced stirrups over h, $1.5 \cdot h$ or $2.5 \cdot h$ respectively in the zone where the plastic hinge will appear. A numerical example is given in table 1 for the ultimate limit angles.

ϑ_u [rad]	Deformation case	A	B	C	D
$\ell/h = 5$	$\ell_p = h$	0.014	0.024	0.022	0.020
	$\ell_p = 2 \cdot h$	0.026	0.040	0.035	0.029
$\ell/h = 10$	$\ell_p = h$	0.018	0.030	0.027	0.024
	$\ell_p = 2 \cdot h$	0.029	0.049	0.045	0.040

Table 1   Ultimate angles for $\ell/h = 5$ and $\ell/h = 10$ with $\psi = 0.8$, $h/r_u = 0.0250$ and $h/r_e = 0.0025$

In most practical cases the slenderness ratio of reinforced concrete columns in buildings is such that the second order effects do not have to be considered. The deflection of the column axis is normally so small that the remaining resistance in the plastic hinge is sufficiently large to balance the moment due to the deflection. When not considering any second order moment, the maximum normal force is equal to

$$N_u = (A_c' - A_s) \cdot f_{ck} + A_s \cdot f_{yk} \tag{2}$$

with A_c' equal the section area of the column without any concrete cover.

2.2 Serviceability limit state

It is evident that the verification of the serviceability has to be based on conventional simple criteria. There are two criteria for the serviceability limit state as follows

a) limitation of the crack widths,
b) prevention of the spalling of the cover concrete.

In order to simplify the verification of these criteria it is sensible to examine only the normal force due to the permanent loads. The imposed angle on the other hand will be estimated with respect to the admissible deflections of the slab and the relatif change in the length of the slab due to the influence of temperature and shrinkage. These imposed deformations are assumed to be time dependent and proportional to that of creep, i.e.increasing from zero at time t = 0 to a final value at time t = ∞.
The second criteria may be neglected since the stresses are in fact positively influenced with time by the nonlinear creep of the concrete which greatly diminishes the danger of concrete spalling at the edge or corner of the column.

The first criteria, the limitation of the crack width,will now be discussed. In this case, the curvature distribution over the column length has to be determined. It can be distinguished between cracked zones (state II) and uncracked zones (state I) in a column. The creep coefficient φ and the age coefficient χ have to be known in order to determine the curvatures. Furthermore, shrinkage (ε_{cs}) has to be considered in state II and a suitable moment-curvature relationship for a constant normal force, such as given in [3] and shown in Fig. 6, has to be used for the analysis. The curvature distribution at time t = ∞ in a column (Fig. 7) can thus be established with the help of design charts.

Fig. 6 Normal Force−Moment− Curvature Relationship :
       (Serviceability State)
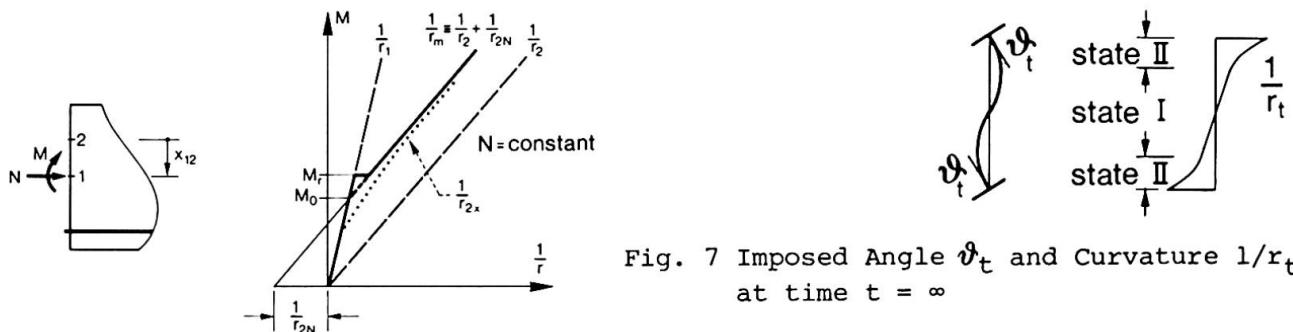
Fig. 7 Imposed Angle ϑ_t and Curvature $1/r_t$
        at time t = ∞

The estimation of the maximum crack width is difficult in a column subjected to a constant normal force and an imposed curvature which reaches at time t = ∞ the value $1/r_t$. It is important to note that the cracks open considerably further with time. A whole series of tests on reinforced concrete slabs subjected to permanent loads, which has been made at the Swiss Federal Institute of Technology, Lausanne, has shown that the crack widths increase by a factor 2 during one year [4], which is a problem of pure bending. Tests have also been made on columns (see chapter 3) in order to study their crack behaviour. A constant normal force with a fixed eccentricity was applied to the columns of the long term load test series. Once again, a net increase of the crack widths was observed. Most existing formulae for the calculation of crack widths do not take into account this phenomenon or if so, very slightly. Furthermore the steel strain ε_{s2} remains more or less constant, at least in the case of pure pending, which makes it even more

difficult to explain adequately the increase in the crack widths. The reasons may lie in the shrinkage of the concrete which is under tension, in the diminishing adherence due to creep, or in the complexe, three dimensional behaviour of the concrete between two cracks.

The following approach, described in detail in [5] is proposed in order to take into account the increase of the crack width with time:

The curvature distribution $1/r_t$ is determined from the given constant normal force N and the given end rotation ϑ_t. With N and $1/r_t$, one determines the moment M. Assuming that M acts already at time t = 0, one determines then $1/r_o$, x_o and $\varepsilon_{sm,o}$, which allows the estimation of the mean crack width

$$w_o = \varepsilon_{sm,o} \cdot (h - x_o)$$

where $\varepsilon_{sm,o}$ is equal to the mean strain in the steel at time t = 0 [3], x_o is equal to the compression zone in the cross section at time t = 0 and $h - x_o$ is equal to the distance between two cracks, assumed to be equal to the length of the tensile zone (St.Venant's principle).

The maximum mean crack width at time t = ∞ is equal to:

$$w_t = \frac{h - x_t}{h - x_o} \cdot \frac{1/r_t}{1/r_o} \cdot w_o$$

The index 0 indicates time t = 0, the index t time = ∞

3. LABORATORY TESTS

Two series of 9 columns of 2.30 m length and with a rectangular section of 0.30 x 0.30 m have been tested under long term loads at EPF Lausanne in order to establish the normal force-moment-curvature relationships at the service limit state. The columns of series A had a constant reinforcement ratio of ρ = 1%. The columns were subjected to a constant normal force of 262 kN to 785 kN with a uni- axial eccentricity varying from 65 mm to 198 mm (Table 2). The deformations of the columns have been observed over a period of one year. Fig. 8 and 9 show the test assembly. The columns of serie B had a reinforcement ratio varying between ρ = 0.50% and 4.72%. All columns were loaded with the same normal force of 523 kN. The eccentricity varied from 100 mm to 221 mm.

The test results of the two series A and B will be published in a test report [6] and in spezialised papers. Fig. 10 shows as an example without any detailed comment the increase of the curvatures in the columns with time.

Other tests have been made on prefabricated centrifuged columns in order to study the ultimate limit behaviour of columns with a high degree of reinforcement. The columns have been tested at EPF Lausanne in collaboration with GRAM SA, Villeneuve, Switzerland, which produces and sells such columns. The 10 columns which have been tested have a diameter of 0.29 m. Six columns have a longitudinal reinforcement of 8 bars of 34 mm (ρ = 12.4%) and four have a HEM 140 steel section in the in- terior (ρ = 18.0%). The columns have been tested in a 10'000 kN press (Fig. 11 and 13) which allows deformation controlled loadings. The load was applied either using inclined steel plates (imposed angle on the columns: 0.01 to 0.02 rad) or linear knife edges (eccentricity: 30 or 60 mm).

The test results [6] demonstrate the high load capacity of centrifuged columns as well as a high degree of ductility which allows to accommodate the imposed deformations.
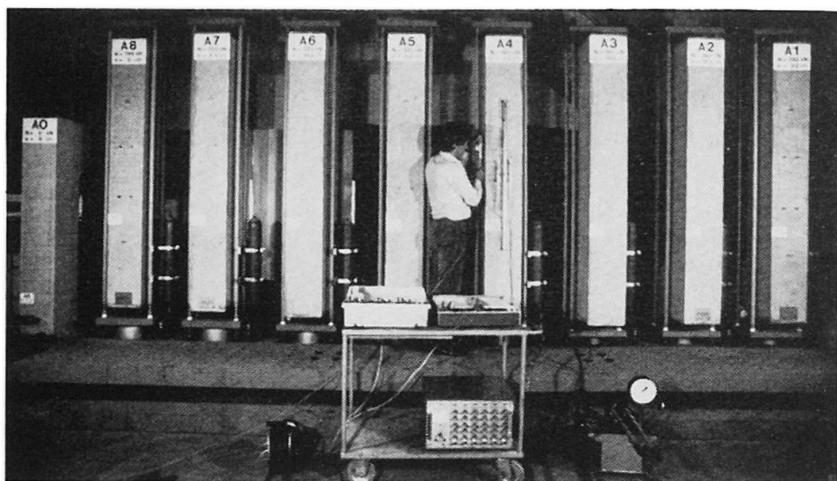
Fig.8 Tests under Long Term Loads
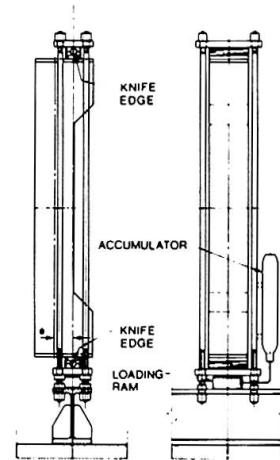
Fig.9 Testing Arrangement

SERIE A		A0	A1	A2	A3	A4	A5	A6	A7	A8
REINFORCEMENT	%	1.00	1.00	1.00	1.00	1.00	1.00	1.00	1.00	1.00
NORMAL FORCE	KN	-	262	262	262	523	523	523	785	785
ECCENTRICITY	MM	-	92	145	198	72	93	113	65	-
B. MOMENT	KNM	-	24.1	38.0	51.9	37.7	48.6	59.1	51.0	

SERIE B		B0	B1	B2	B3	B4	B5	B6	B7	B8
REINFORCEMENT	%	-	0.50	0.50	2.26	2.26	4.72	4.72	-	-
NORMAL FORCE	KN	-	523	523	523	523	523	523	523	1134
ECCENTRICITY	MM	-	109	123	129	156	161	221	100	-
B. MOMENT	KNM	-	57.0	64.3	67.5	81.6	84.2	115	52.3	-

Table 2 Loads of the Test Columns

Fig.10 Curvatures against Time
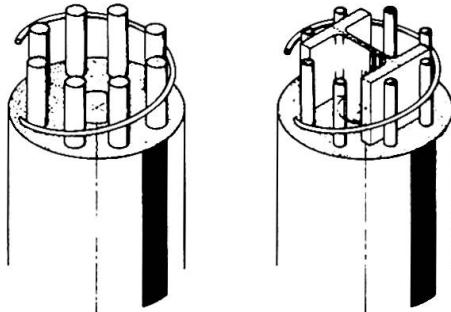
Fig.12 Two Column Types
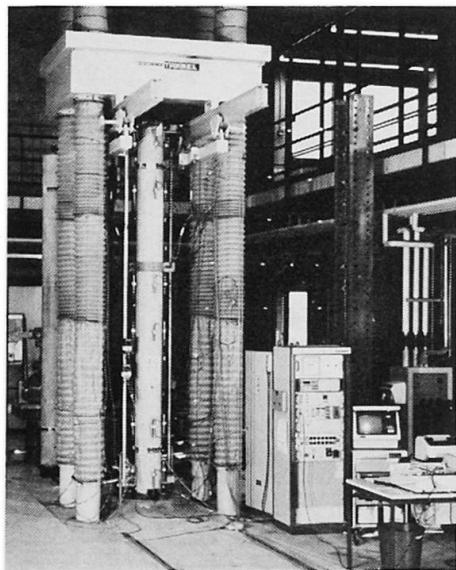
Fig.11

Test assembly
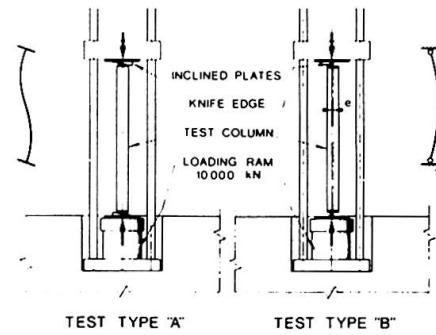
Fig.13 Deformation Cases

4. EXAMPLE

Consider a column with a length of 3.50 m, adequtately confined with reinforcement as shown in Fig. 14. The slabs impose on the column the usual type of deformation, type D, Fig. 3.
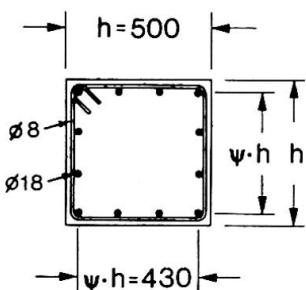
Fig. 14 Cross Section
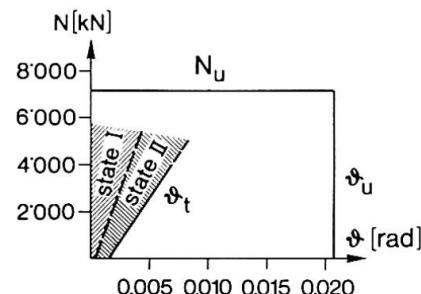
Fig. 15 Ultimate and admissible limit angle

The degree of reinforcement is equal to 12 bars of $\emptyset$ 18, ρ = 1.2 %, where A_s = $3 \cdot 10^3$ mm^2. The stirrups of $\emptyset$ 8 have a spacing of 50 mm over a length of 750 mm at the column ends and of 200 mm elsewhere. The concrete grade is C 30 with a compressive strength f_{ck} = 30 N/mm^2 and a tensile strength of 2 N/mm^2. The creep coefficient is equal to φ = 2.5, the age coefficient χ = 0,8 and the value for shrinkage may be taken as ε_{cs} = 25 $\cdot$ 10^{-5}.

The determination of the limit angles is required as a function of the normal force N which the column is able to support at the ultimate and serviceability limit state.

Solution : The slenderness ratio is with $\lambda = \sqrt{12} \cdot \ell/h$ = 24 very small. The influence of second oder does not need to be checked. Equations (1) and (2) give

$$\vartheta_u = 3.5/6 \cdot 0.5 \cdot 0.0025 + (1 - 0.5/3.5) \cdot (0.0233 - 0.0025) = 0.0207 \text{ rad.}$$

$$N_u = (450^2 - 3000) \text{ mm}^2 \cdot 30 \text{ N/mm}^2 + 3000 \text{ mm}^2 \cdot 400 \text{ N/mm}^2 = 7185 \text{ kN}$$

with $\lambda_p = \ell_p/h$ = 1, h/r_e = 0.0025 (from design chart) and h/r_u = 0.0233.

An even higher ultimate angle could be reached if one provides the column with closely spaced stirrups over a larger length than has been assumed. No failure occurs in a column subjected to a normal force N smaller than N_u = 7185 kN if the imposed angle is smaller than ϑ_u = 0.0207 rad (see Fig. 15). The assumption of a maximum mean crack width w_m = 0.2 mm leads to the limit angle ϑ_t for the serviceability state. The dotted line in Fig. 15 represents the limit angle so that no cracks occur in the column assuming $\sigma_c = f_{ct}$ = 2 N/mm^2.

5. REFERENCES

[1]   SCOTT B.D., PARK R. and PRIESTLEY M.J.N., Stress-Strain Behaviour of
       Concrete Confined by Overlapping Hoops at Low and High Strain Rates. ACI
       Journal, Title no 79-2, Jan-Feb 1982.
[2]   THÜRLIMANN C., Bemessung von Stahlbetonstützen unter Zwangsverformungen
       (Design of R.C. Columns under Imposed Deformations). PhD Dissertation,
       Swiss Federal Institute of Technology Lausanne, 1984.
[3]   CEB-MANUEL, Cracking and Deformation, Lausanne 1983.
[4]   JACCOUD J.-P., FAVRE R., Flèches des structures en béton armé
       Annales de l'JTBTP, Paris, 1982.
[5]   NAJDANOVIC D., Vérification de l'état d'utilisation des colonnes sous
       l'effet de déformations imposées de longue durée. PhD Dissertation,
       Belgrade and Lausanne, to be published in 1985.
[6]   SUTER R., DAL BUSCO S. Test reports, Inst. of Technology, Lausanne 1984.

# Towards a Consistent Design of Reinforced Concrete Structures

Dimensionnement unitaire des structures en béton armé

Zum einheitlichen Bemessen von Stahlbetontragwerken

Jörg SCHLAICH
Prof. Dr.
Stuttgart, Fed. Rep. of Germany
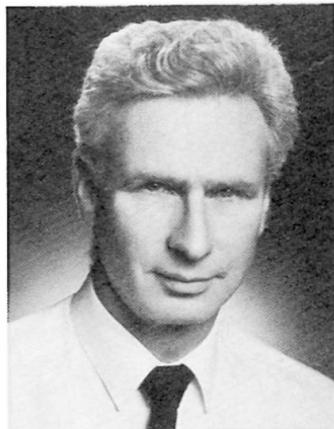
Jörg Schlaich, born 1934. Studies of architecture and civil engineering at Stuttgart, Berlin and Cleveland, Ohio. Professor at the Institut für Massivbau, University of Stuttgart. Partner of Schlaich & Partner, Consulting Engineers, Stuttgart.

Kurt SCHÄFER
Prof. Dr.
Univ. of Stuttgart
Stuttgart, Fed. Rep. of Germany

Kurt Schäfer, born 1936. Study of civil engineering at Karlsruhe, FRG. Research Associate at Stanford University, California. Structural Engineer with different companies. Professor at the Institut für Massivbau, University of Stuttgart.

SUMMARY

The truss model developed by Ritter and Mörsch for the design of shear reinforcement is a simple tool for explaining the internal forces in beams. It is generalized here for application to other reinforced concrete structures. Suggestions are made for the design of all members and nodes of such generalized strut models according to unified principles. Thus a consistent design concept for all kinds of reinforced concrete structures is achieved. This could be the basis for a better understanding of reinforced concrete and for simpler codes.

RESUME

Le modèle en treillis développé par Ritter et Mörsch pour le dimensionnement des armatures à l'effort tranchant dans des poutres est un moyen simple pour illustrer la distribution des forces intérieures. Il est généralisé et appliqué aux autres structures et éléments en béton armé. Si les membres et les noeuds sont dimensionnés sur la base des principes unitaires suggérés, il devrait être possible d'arriver à une conception universelle pour le dimensionnement de structures en béton armé. Cela pourrait conduire à un code plus simple et à une meilleure compréhension du béton armé.

ZUSAMMENFASSUNG

Die Fachwerkanalogie von Ritter und Mörsch liefert ein einfaches Modell zur Beschreibung des Kraftflusses in Stahlbetonbalken. Sie wird verallgemeinert und auf andere Tragglieder und Tragwerksbereiche angewendet. Wenn nun, wie vorgeschlagen, alle Stäbe und Knoten der verallgemeinerten Stabwerkmodelle nach einheitlichen Gesichtspunkten bemessen werden, kommen wir zu einem einheitlichen Bemessungskonzept für den ganzen Stahlbetonbau. Dieses könnte auch die Grundlage für ein besseres Verständnis des Stahlbetons und für einfachere Normen sein.

The ideas in M. Wicke's paper in the introductory report for this con-
ference ("Developments in the Design of Reinforced and Prestressed Con-
crete Structures") are further elaborated in the following.

1. THE STRUCTURE'S B- AND D-REGIONS

Those regions of our structures, in which the Technical Bending Theory's
assumption of plane strain is good enough, we nowadays design with an almost
exaggerated care and "accuracy" by standard methods. We suggest to call them
B-regions   (B stands for beam and bending). Their internal state of stress is
rapidly derived from the sectional forces and moments.

Standard methods are not applicable to all the other regions and details of a
structure where the strain distribution is nonlinear e.g. near concentrated
loads, corners, bends, openings, etc. (fig. 1). These we call D-regions (D for
discontinuity, disturbance, detail). The D-regions are as equally important for
the safety and serviceability of a structure as the B-regions, but are mostly
designed and reinforced according to rules of thumb or on a purely experimental
basis. This is obviously one of the sources of damage that is frequently found
in D-regions.
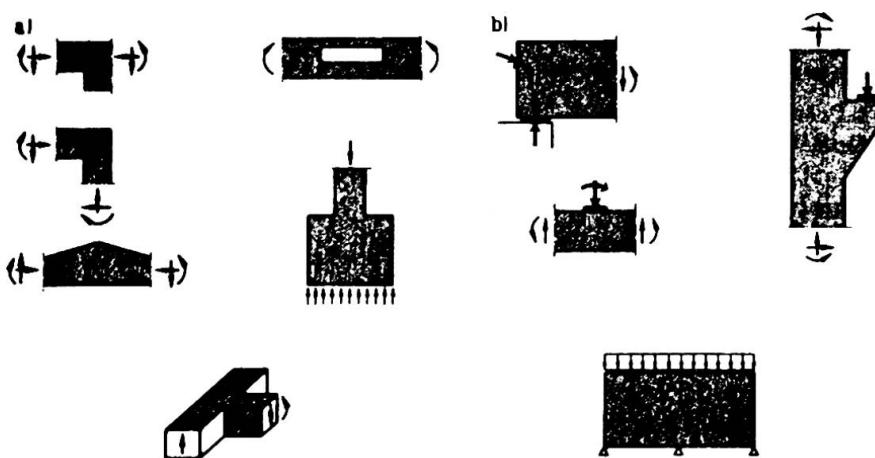
Fig. 1 (a) Geometrical discontinuities, (b) statical and/or geometrical
      discontinuities

A design concept should be clear and based on simple models in order to avoid
rules which are not understood by the designing engineer. A consistent design
concept must comprise B- and D- regions without contradictions. Considering the
complexity of B-region design and the even more complex state of stress in D-
regions a unified design concept will require concessions with respect to ac-
curacy. But we think even a very simplified methodical concept will be better
than todays practise of D-region design.

For this purpose it is suggested to generalize the well known truss analogy
for beams (fig. 2) in order to apply it in form of generalized strut models to
the more complicated regions and to the whole structure /1-3/. The strut model
condenses all stresses in tension and compression members which are connected
by nodes. If we design all its members and nodes with uniform criteria, we
arrive at a consistent design concept which is applicable to all possible cases.
On top of that it could be the basis for a better understanding of reinforced
concrete and therewith for better and safer structures and simpler codes.
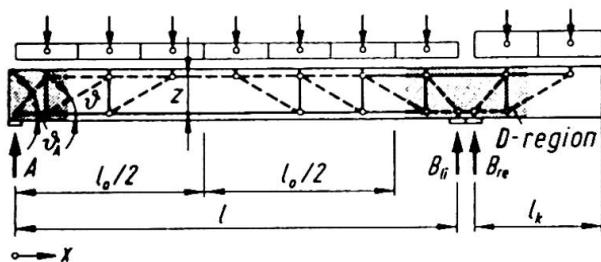
Fig. 2 Truss model of a beam
with cantilever
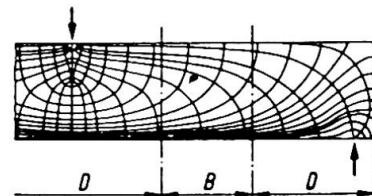
Fig. 3 Stress trajectories
near discontinuities

Stresses and stress trajectories are quite smooth in B-regions compared to their turbulent pattern near discontinuities (fig.3). Stress intensities decrease rapidly with the distance from the origin of stress concentration. This behaviour allows us to classify B- and D-regions by splitting the real state of stress (fig. 4a) into two states:

The state of stress (b) complies with Bending Theory. It has to satisfy equilibrium between external loads and reactions, but may violate the actual boundary conditions.

The superimposed state of stress (c) is necessary in order to satisfy the boundary conditions. The applied group of forces is self-equilibrating. According to the principle of De St.Vénant the stresses are negligible in a distance from the equilibrating forces, which is approximately equal to the distance between the forces themselves. It defines the D-regions. However, cracked concrete members have different stiffnesses in different directions; this enlarges the D-regions in the direction parallel to the cracks considerably, which may be taken into account. The subdivision of a structure into B- and D-regions is already of considerable value for the comprehension of the internal forces in the structure. The method is applied to a frame in fig. 5.
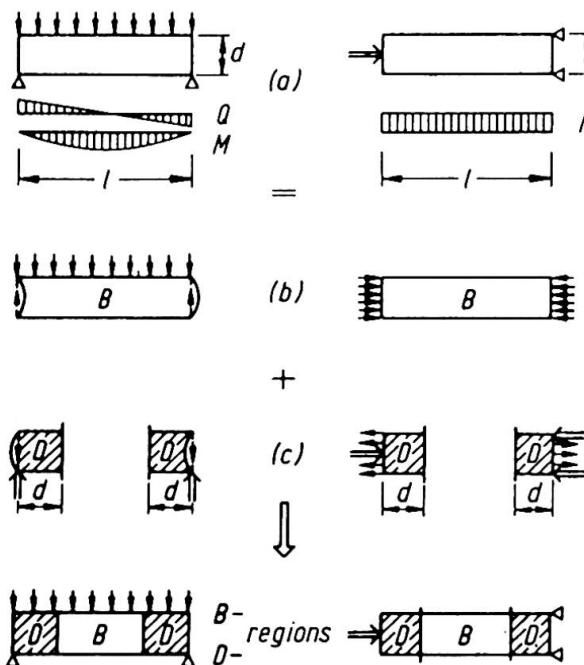
Fig. 4 Splitting of structure
into B- and D-regions
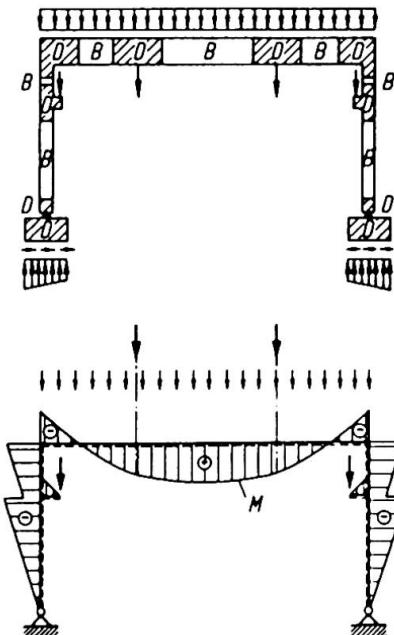
Fig. 5 Frame structure
with B- and D-regions

2. MODELLING

We suggest the following basic procedure for the design with truss or strut models (fig.6):
- develop the geometry of the model by orienting the struts and ties at the stress trajectories for elastic behaviour considering the material properties, especially stiffnesses, and the detailing of reinforced concrete;
- calculate the member forces, fulfill equilibrium;
- dimension the members and nodes:
  check capacity of compression members and of possible unreinforced tension members, design reinforcement of tension members with due consideration of crack limitations.

This method implies that the structure is designed according to the lower bound theorem of plasticity. As concrete allows only limited plastic deformations the internal structural system (the strut model) has to be chosen in a way that the deformation limit (capacity of rotation) is not exceeded at any point before the assumed state of stress is reached in the rest of the structure.

This requirement is automatically fulfilled by adapting the strut model and reinforcement to the direction and size of the internal forces as they would appear from the theory of elasticity. In highly stressed D-regions we propose to proceed accordingly. In medium or minor stressed D-regions even large deviations from the ideal reinforcement pattern are no problem as the structure adapts to the assumed internal structural system. However, a minimum reinforcement which is sufficient to control crack widths has to be provided.
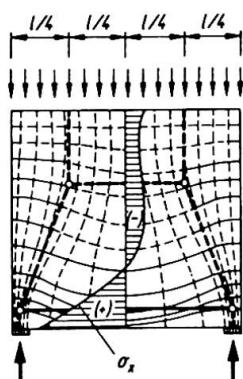
Fig. 6 The strut model approximating the stress trajectories

Whoever spends some time with developing strut models will make the useful and instructive observation that some types of D-regions appear over and over again even in the apparently most different structures. As an example fig. 7 shows D-regions in 4 different structures, altogether modelled with the same type of model (fig.6): A detail of internal forces in a beam, the distribution of cable forces in a bridge deck, a wall with big openings and a box girder with anchor loads from prestressing tendons. In all of these cases the pattern of internal forces is basically identical.

With an unlimited number of examples it could be shown, that tracking down of the internal forces by truss models results in safe structures and quite often provides simple solutions for problems which seem to be rather complicated or reveal weak points which were not obvious. Let us investigate just two examples:

It is well known, that the support reaction A of the beam in fig. 8 must be suspended beside the recess. But the complete strut model reveals clearly, that this is not sufficient: The stirrups have to carry approximately 1,5 A, for the geometrical configuration given. And stirrup stresses may increase furthermore with an additional horizontal reaction at the support.

The girder in fig. 9 obviously produces a vertical tension force T at the bend
of the compression cord. But where does it go? The straight horizontal tension
cord cannot equilibrate it. The model a) shows, that stirrups in the web are
necessary throughout this web with zero shear force. Looking at fig. 9b we
realize, that the compression cord is narrowed by the stirrups, resulting in a
concentration of compression stresses over the web. Furthermore, tensile
stresses in the transverse direction of the flange appear.
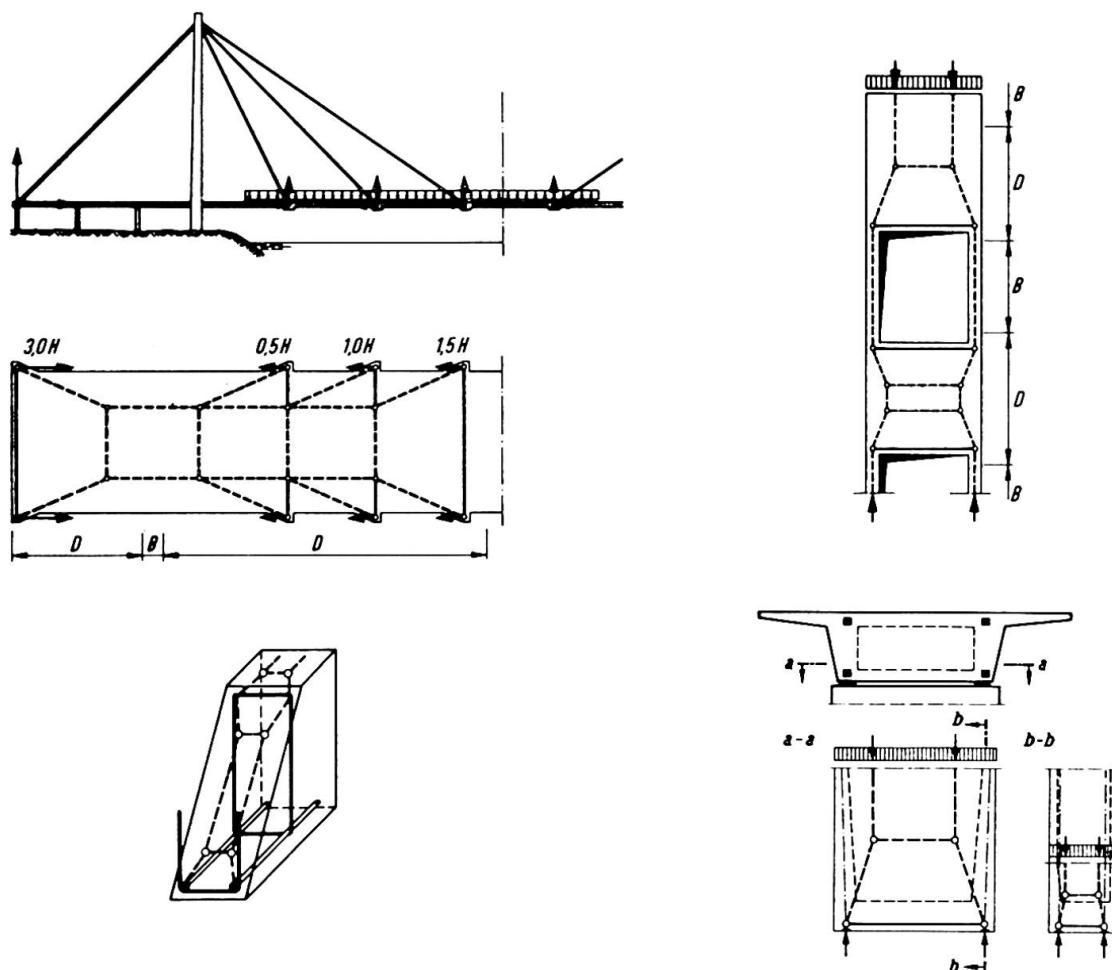
Fig. 7 One single type of a D-model appears in 4 different structures

Fig 8 Beam supported in a recess
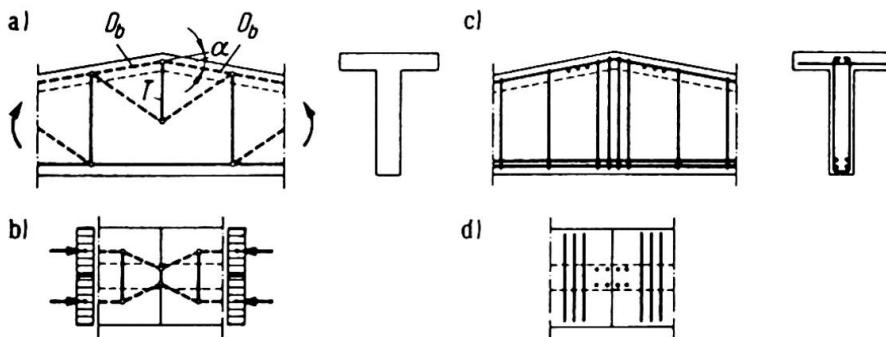
Fig. 9 Girder with
bent top flange

3. DIMENSIONING

After a suitable strut model is found, its individual members and nodes have to be designed for the forces they carry. Tension members in the model will pose no problems, if we provide reinforcement or prestressing for the tension force.

However, in many cases we have to introduce tension members into our models in such places where normally no reinforcement is positioned or cannot be inserted for practical reasons. It is one of the advantages of the proposed procedure to reveal in which places the equilibrium of a structure relies on the tensile strength of the concrete. No lap splice, no bond anchor, no frame corner, no plate without shear reinforcement, not even a compression bar could work without the tensile strength of the plain concrete. If we are striving for a unified design concept and want to simplify our codes, we should not deny the concrete tensile strength and refer to it obliquely by terms such as bond or shear. Instead we must introduce and specify the tensile strength as a design quantity.

We propose to use the RVE method (representative volume element) as a practical means of smoothening out stress peaks. Thereby all kinds of tensile stress distributions can be judged by comparison with one single material property, the tensile strength of axially loaded prisms. However, the tensile strength of the concrete may be utilized for maintaining equilibrium only in such cases, where local cracking does not cause progressive failure of the whole tension zone. Existing microcracks from secondary stresses and local faults from concreting could be taken into account by assuming a representative fault area of e.g. $A = 4\ d_K^2 = (d_K = $ maximum aggregate size).

The compression bars of our model are in reality 2 or 3-dimensional stress fields. The compression stresses are constricted near the nodes and spread out in between, thereby creating transverse compression and tension stresses. If we characterize the geometry of a plane bar by an effective width b_{ef} and node dimensions a_1, a_2 (fig. 10) a conservative value of the bar's critical load krit F can be taken from fig. 11. The continous lines give the average σ_0 and p_a at failure of the compression bar due to transverse tension. The broken lines are postulated upper bounds for the stresses p_a in plane and 3-dimensional stress fields, respectively.
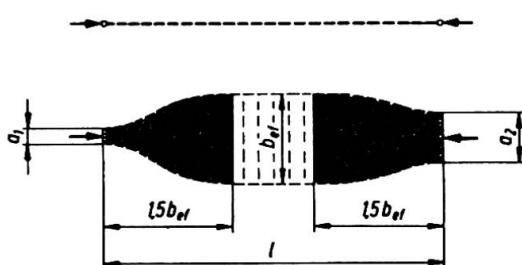
Fig. 10 The compression bar

This concept of dealing with compression in concrete obviously covers standard cases of design, e.g. compression cords of beams and locally loaded concrete as well as the many cases where no generally agreed upon method for the design of compression zones exists, as for corbels, frame corners, deep beams etc. The concept is also applicable to the design of compression struts in beams which today implicitly is taken care of by allowable shear stresses.

The nodes are indispensable parts of the structure. The strut forces resp. stresses are applied at the periphery of the nodes. Although there exist many different types of nodes the balance of the forces takes place in most cases in a concrete node region stressed by compression only (fig.12). The design of these nodes becomes very simple, if a hydrostatical state of stress is assumed in the node region, which means equal stresses in all directions of the struts. The hydrostatical state of stress can be plane or three-dimensional according to the type of the node. The width of the struts at the node are then directly proportional to their forces. From this it becomes clear that there is a close relation between the structural detail, i.e. the design of the nodes and the dimensions resp. capacities of the compression bars. Fig. 13 shows a corbel as an example which can be designed completely with this method.
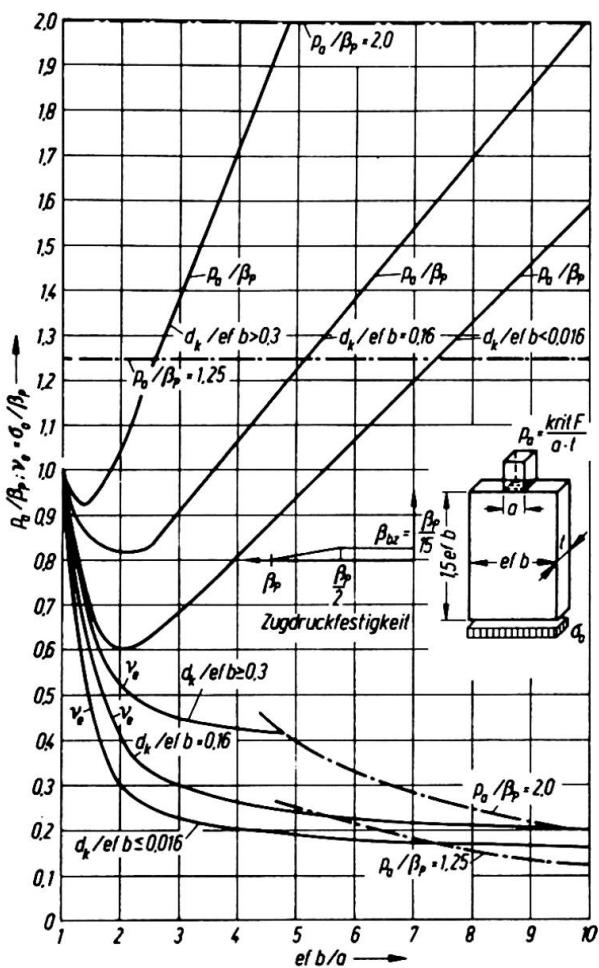
Fig 11 Diagram for evaluating the
critical load of

plane compression bars

(β_p = prism strength)
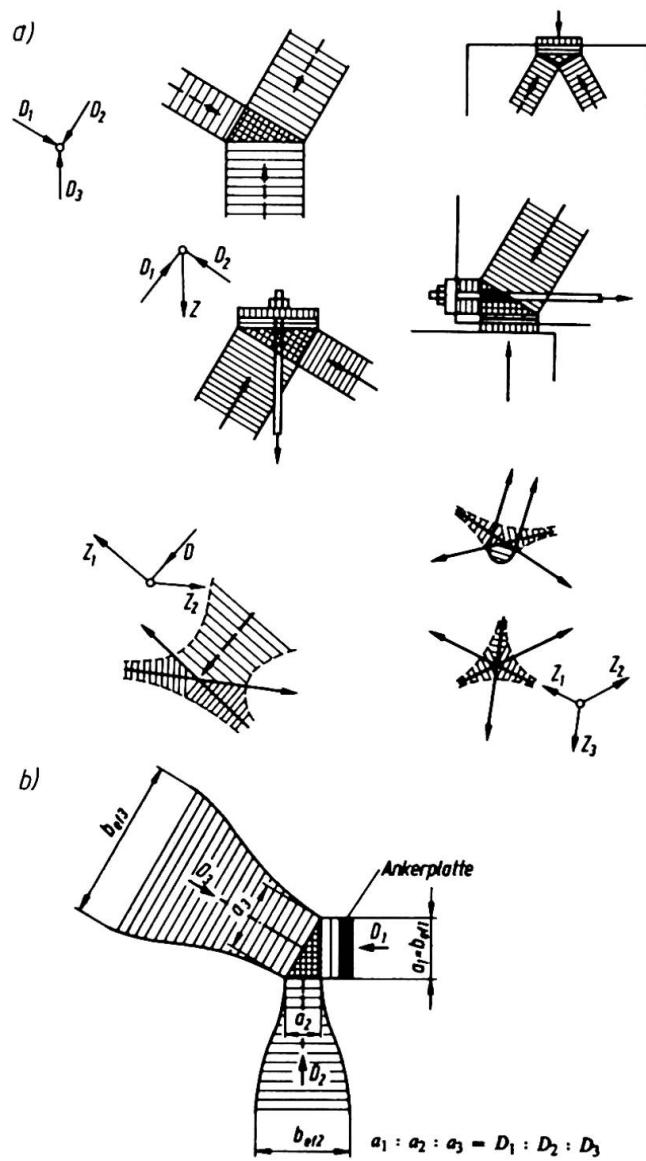
Fig. 12 (a) Different types of nodes

(b) Node with hydrostatic stress
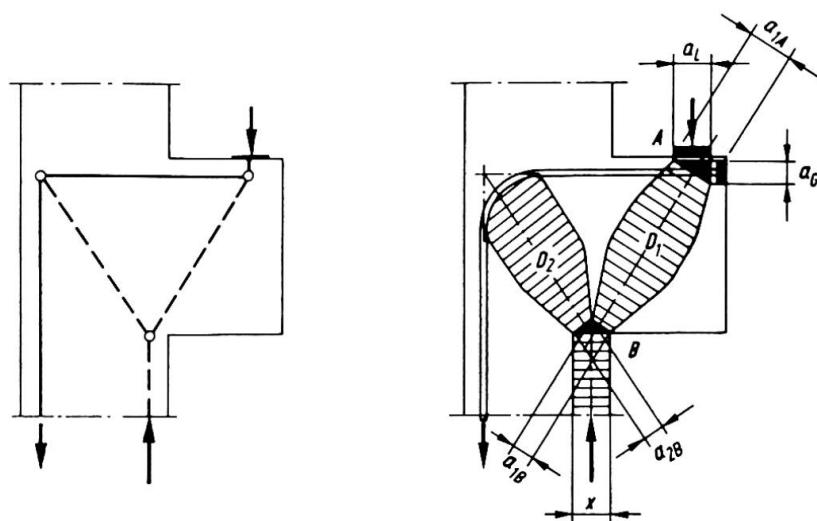
Fig. 13 Compression bars (fields) of a corbel

4. CONCLUSIONS

Calculations with the described strut models and comparison with experimental results show that this method is not only simple and clear but also leads to sufficiently accurate results.
If the design concept developed for the D-regions is applied to the B-regions it is able to explain also their well known behaviour. For example it can be shown that the low stirrup stresses in the low shear range are a consequence of the tensile strength of the concrete. Furthermore a close look at B-regions (e.g. beam section in fig. 7) discloses micro D-regions within the B-regions, where the method again is applicable and reveals for example the influence of detailing and spacing of stirrups on the load carrying capacity of B-regions. Many of the empirically derived code rules could be abandoned or improved by consistent application of the described method, but this is beyond the scope of this paper and was discussed elsewhere /1-3/.

Therefore it is felt that a consistent design concept for all kinds of r.c. structures and details can be developed. This could become the basis for a better understanding of reinforced concrete and for simpler codes.

References:

1   Thürliman et al: Anwendungen der Plastizitätstheorie auf Stahlbeton.
     Vorlesung zum Fortbildungskurs für Bauingenieure. Institut für Baustatik
     und Konstruktion. ETH Zürich 1983

2   Schlaich, J., und Weischede, D., Ein praktisches Verfahren zum methodischen
     Bemessen und Konstruieren im Stahlbetonbau. Bulletin d'Information N⁰ 150.
     Comité Euro-International du Béton, März 1982.

3   Schlaich, J., und Schäfer, K., Konstruieren im Stahlbetonbau. Beton-Kalen-
     der Teil II, Berlin-München: W.Ernst & Sohn 1984, p. 787-1005.

Expérimentation d'une structure treillis en béton

Versuche an Fachwerkelementen aus Beton

Test Loading of a Concrete Truss

Jean BRUNEAU
Ing. Ponts et Chaussées
DRE
Ile de France

Né en 1948, ancien élève de
l'Ecole Polytechnique et de
l'Ecole Nationale des Ponts et
Chaussées. Pendant 5 ans, il a été
responsable d'essais de structures
au Laboratoire Central des Ponts
et chaussées. Actuellement, il est
responsable d'études et de réali-
sation d'ouvrages d'art en Région
Ile de France.

Gilles CAUSSE
Ing. Ponts et Chaussées
SETRA
Bagneux, France

Né en 1956, ancien élève de
l'Ecole Polytechnique et de
l'Ecole Nationale des Ponts et
Chaussées. Il est chef d'arron-
dissement à la Division des
Ouvrages d'Art du SETRA de-
puis 1980.

Bernard RASPAUD
Dir. Etudes Adj.
Bouygues
Clamart, France

Né en 1942, de formation uni-
versitaire et diplôme du CHEBAP,
il rejoint le Groupe Bouygues en
1972, après 4 ans passés à la
Direction Départementale de
l'Equipement de la Seine Saint-
Denis. Depuis 5 ans, il dirige le
bureau d'Etudes de Bouygues
Travaux Publics.

Bruno RADIGUET
Ing. Chef de Groupe
Bouygues
Clamart, France

Né en 1948, diplômé de l'Ecole
Centrale de Paris. Il s'est con-
sacré depuis 1972 aux études
d'ouvrages d'Art, au sein du
Groupe Bouygues. Il a participé,
en particulier, aux études du
pont de Bubiyan.

RESUME
Il a été procédé, en 1982, à l'occasion des travaux du pont de Bubiyan au Koweit, à une expérimenta-
tion sur un modèle à l'échelle I. Des essais de chargements, ont montré un fonctionnement validant des
méthodes de calcul simplifiées. Les mesures réalisées par extensométrie au moyen de jauges résistives,
ont mis en évidence un bon accord entre l'expérience et les calculs.

ZUSAMMENFASSUNG
1982, aus Anlass des Baus der Bubiyan-Brücke, wurden Modellversuche im Massstab 1:1 durchgeführt.
Die Belastungsproben zeigten die Gültigkeit der vereinfachten Berechnungsverfahren. Die Dehnungs-
messungen zeigten, dass eine gute Übereinstimmung zwischen Versuch und Berechnung besteht.

SUMMARY
In 1982, in conjunction with its Bubiyan Bridge construction project in Kuwait, the Bouygues company
conducted a series of test loadings on a full-scale test model. Loads were applied by means of concrete
blocks and vertical prestressing bars. Results confirmed the validity of simplified calculation methods;
extensometric readings obtained from resistance strain gauges showed agreement between theoretical
and actual values.

1   PRESENTATION

1.1. Cadre de l'opération

C'est en Novembre 1980 que l'Entreprise BOUYGUES soumet au gouvernement du Koweit son offre concernant une solution variante du pont de BUBIYAN. La structure proposée (treillis tridimensionnel en béton, précontraint extérieurement) est finalement retenue à l'issue d'une rude compétition internationale.

Parallèlement, et avec l'appui du SETRA, l'Entreprise dépose une demande de prêt, qui sera acceptée, auprès de l'ANVAR (Agence Nationale pour la Valorisation de la recherche), afin de réaliser une expérimentation sur ce type de structure.

La réalisation du modèle d'essai commence à l'automne 1981 avec la collaboration du SETRA pour les calculs de la structure, et l'intervention du Laboratoire Central des Ponts et Chaussées qui confie à la Direction Régionale de l'Equipement de l'Ile de France et plus particulièrement sa division, le Laboratoire Régional de l'Est Parisien, la réalisation des essais et des mesures.

Les essais sous charges de service ont lieu en mai 1982 et les essais sous surcharges majorées (charges de service multipliées par 2.7) en mai 1983.

1.2. Géométrie du modèle

Afin d'éviter les interprétations, toujours délicates, qui sont nécessaires lorsque l'on conduit des expérimentations sur des maquettes à échelle réduite, c'est un modèle à l'échelle 1 qui a été réalisé. Les dimensions des éléments constitutifs du treillis (dimensions des nœuds, des diagonales et des mailles du treillis) sont donc les mêmes que celles du pont de BUBIYAN.

Le modèle est constitué de 9 voussoirs préfabriqués (6 voussoirs courants, 2 voussoirs sur piles plus massifs et 1 voussoir d'about) ; les diagonales sont en béton armé, sauf certaines diagonales des voussoirs 4 et 5 qui sont précontraintes. Cet ouvrage de 34.72 m de longueur repose sur deux lignes d'appui distantes de 25.18 m ; sa largeur est de 8.64 m. Rappelons ici les objectifs fixés :

— Reproduction fidèle de la structure du pont de BUBIYAN afin de tester certains aspects de la réalisation (coffrage des triangles préfabriqués constituant le treillis ; ferraillage des nœuds ; mise en œuvre des joints secs ...).

— Possibilité de créer, dans les diagonales, des efforts identiques à ceux du pont de BUBIYAN sous charges de service et sous surcharges majorées, en vue d'une étude sous fissuration, afin d'établir une comparaison avec les résultats de calcul.

1.3. Chargement de la structure

Trois types de charges ont été utilisés :

— Sachant que la portée des travées de BUBIYAN est de 40.16 m, alors que la portée entre appuis du modèle n'est que de 25.18 m, il est nécessaire, afin de retrouver dans ce dernier les sollicitations de poids propre d'une travée courante de BUBIYAN, d'ajouter des charges permanentes. Pour cela, 3 blocs de 700 KN (2100 KN au total) ont été utilisés.

— Les efforts sous charges de service sont simulés par 9 tirants Dywidag reliant la dalle supérieure au radier de fondation. Ces tirants permettent de mobiliser les 2100 KN représentant les charges de service ; mais en outre, leur capacité allant jusqu'à 3300 KN, ils sont utilisés pour simuler une part des surcharges majorées. Les vérins de ces barres sont contrôlés par des jauges de déformation permettant une vérification à 2 % près de la tension.

— Enfin, 6 blocs de 400 KN (2400 KN au total) complètent le chargement sous surcharges majorées.

1.4. Instrumentation

1.4.1. Généralités

Les techniques mises en œuvre sont classiques. Les mesures de déformation sont obtenues par jauges résistives fixées sur les aciers et sur le béton. Des mesures de flèches viennent les compléter à chaque stade de chargement. En outre, les relevés de la température extérieure et de la température dans la structure sont effectués simultanément. Les joints de voussoirs (sans colle) sont portés par des capteurs de déplacement permettant de déceler tout mouvement.

Par ailleurs, un relevé de la fissuration par examen visuel est effectué à l'issue de chaque série de mesures. Sur les diagonales tendues en béton armé, le dispositif de mesures locales est complété par des extensomètres à fil de grande longueur de base (2.00 m), destinés à mesurer la déformation moyenne de l'élément, compte-tenu de la fissuration répartie.

Le modèle, situé à l'extérieur, est exposé aux intempéries et au rayonnement solaire. Ceci nécessitait de porter une attention particulière à la protection des jauges. Pour cela, a été mis en œuvre un appareillage de saisie automatique

SECTION TRANSVERSALE

BUBIYAN

MODELE

VUE D'ENSEMBLE

DIAGONALES
BETON
PRECONTRAINT
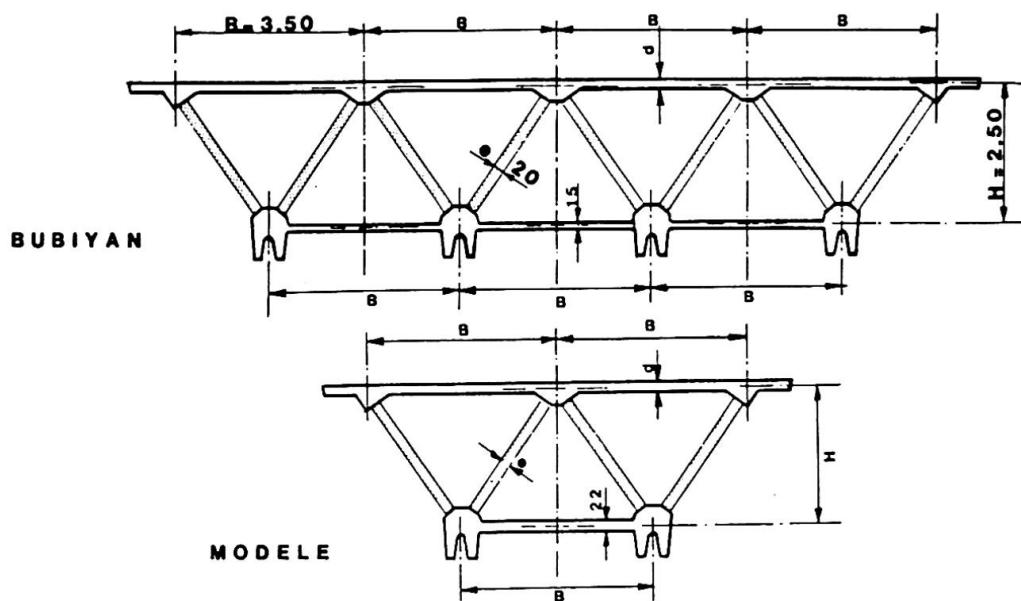
DIAGONALES
BETON ARME
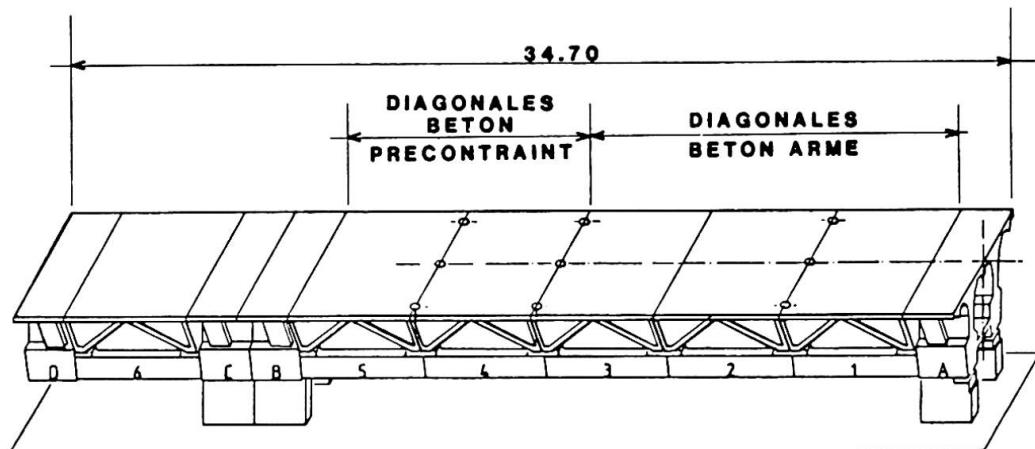
PRECONTRAINTE ET CHARGE PERMANENTE

2 Cables 27T15

2 Cables 27T15

70T   70T   70T
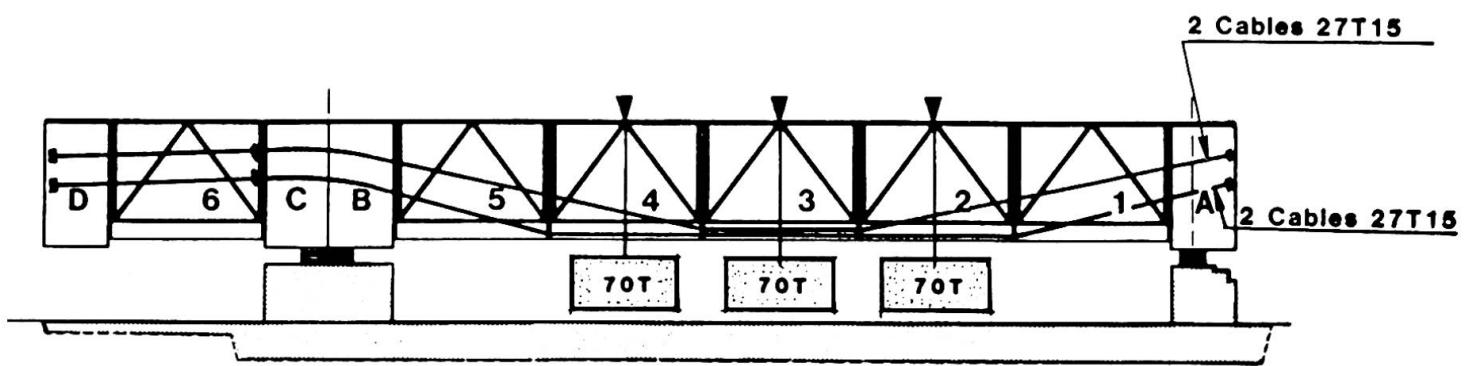
des résultats permettant de limiter la durée des mesures et donc de réduire les dérives des appareils, et en particulier, les dérives thermiques en cours de chargement.

Afin d'estimer les modules de déformation du béton, des éprouvettes sont prélevées lors du bétonnage et testées à chaque série d'essais.

1.4.2. Equipement des diagonales

Chaque diagonale comprend 3 sections de mesures ; deux sont proches des encastrements et sont équipées de jauges longitudinales, la section médiane comportant pour sa part deux jauges sur les faces supérieure et inférieure. Ce dispositif permet de déterminer l'ensemble des déformations longitudinales des sections d'encastrement, et d'en déduire les contraintes normales, puis les sollicitations d'effort normal et de moment de flexion. Deux voussoirs ont été entièrement équipés : le voussoir 1 (diagonales en béton armé) et le voussoir 5 (diagonales en béton précontraint).

L'ensemble du dispositif comprend 350 voies de mesures , jauges, capteurs et sondes de température. Ce dispositif est relié à un sytème de mesure d'enregistrement, couplé à un micro-ordinateur qui permet le stockage et l'édition des résultats.

Trois mesures sont effectuées pour détecter les instabilités. Grâce à l'automatisation du dispositif, 10 minutes suffisent pour l'acquisition de la totalité des mesures.

1.5. Modèle de calcul

Les calculs de l'ouvrage ont été effectués au préalable en utilisant plusieurs modèles de calcul afin d'étudier les différentes particularités de fonctionnement de la structure :

— Tout d'abord, un modèle plan dans lequel chaque barre a une rigidité équivalente à celle de l'ensemble des éléments contenus dans le plan transversal correspondant.

— Ensuite un modèle à trois dimensions, permettant l'analyse du fonctionnement transversal de la structure. Les dalles supérieures et inférieures sont ici modélisées par des plaques d'épaisseur constante, et les nervures longitudinales sont représentées par des barres, rétablissant ainsi la rigidité des hourdis. Enfin, pour les diagonales, c'est la section brute qui est prise en compte.

2 – PRINCIPAUX RESULTATS DE CALCULS ET COMPARAISON AVEC LES VALEURS OBTENUES EXPERIMENTALEMENT

2.1. Comportement d'ensemble de la structure

— La flèche due aux déformations de flexion est extrêmemement proche de celle d'une poutre en I constituée des seules membrures. Cependant, la flèche en milieu de travée due aux déformations d'effort tranchant ne saurait être négligée ; en effet, elle représente ici près de 40 % de la flèche totale.

— La déformabilité sous effort tranchant pur, varie selon que l'on considère les zones proches des appuis ou les zones en milieu de travée. En effet, l'effort tranchant est repris pour partie par la triangulation et pour le reste par les houdis. Or la participation de ceux-ci varie longitudinalement (entre 5 et 25 %) du fait de la nécessité de compatibilité des déformations d'effort tranchant et de flexion.

2.2. Comportements locaux

Les résultats de mesure ont confirmé que les charges concentrées « s'étalent » dans la structure (comme les calculs l'avaient laissé prévoir).

En effet, lorsqu'une charge concentrée est appliquée sur le hourdis supérieur, à un nœud du treillis, on ne retrouve que 60 % de cette charge dans les diagonales partant de ce nœud, les 40 autres pourcents migrant par la dalle supérieure vers les nœuds voisins.

Ceci explique que les moments locaux dans les hourdis soient environ deux fois plus élevés que ceux provenant de la seule courbure longitudinale de la structure.

2.3. Comportement des diagonales

Dans les voussoirs 4 et 5, les diagonales tendues sont précontraintes, on constate un bon accord entre le calcul et les résultats expérimentaux ; les écarts sont au maximum de 7 à 8 %.

Cependant l'interprétation expérimentale des moments locaux des barres conduit à conclure que ceux-ci sont légèrement plus élevés que ceux calculés.

SURCHARGES

CHARGES DE SERVICE

Chargement 1

Chargement 2

Chargement 3

Chargement 4

Chargement 5
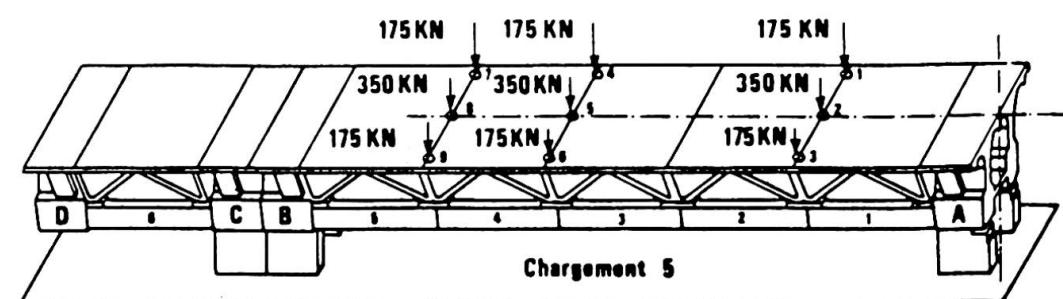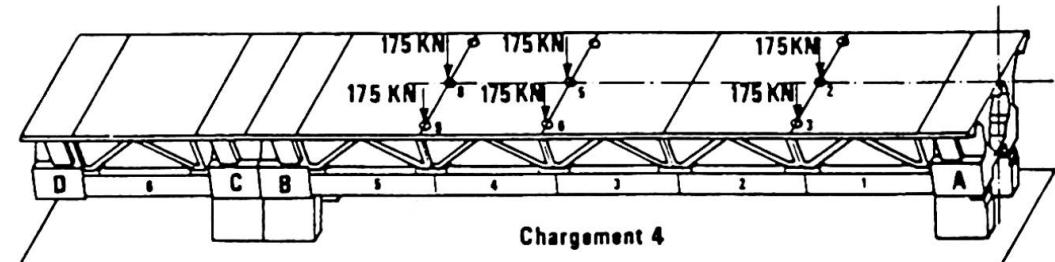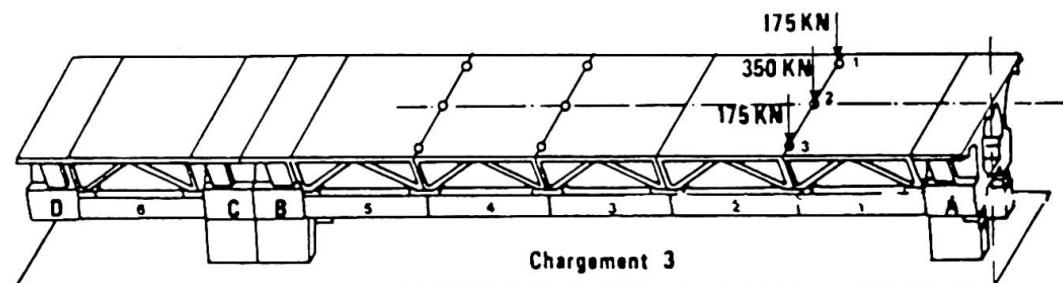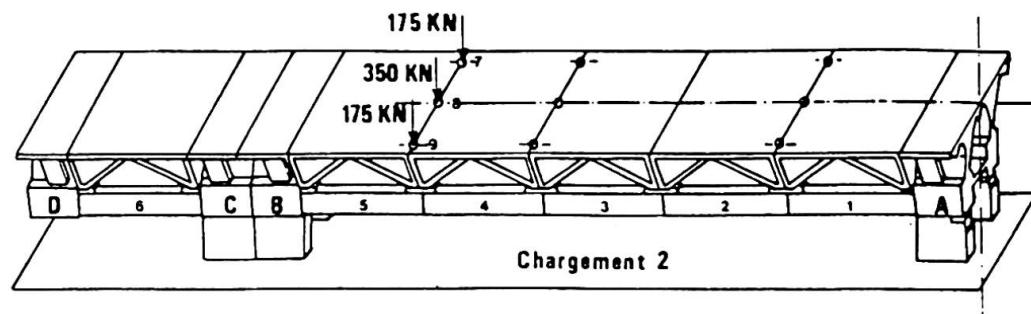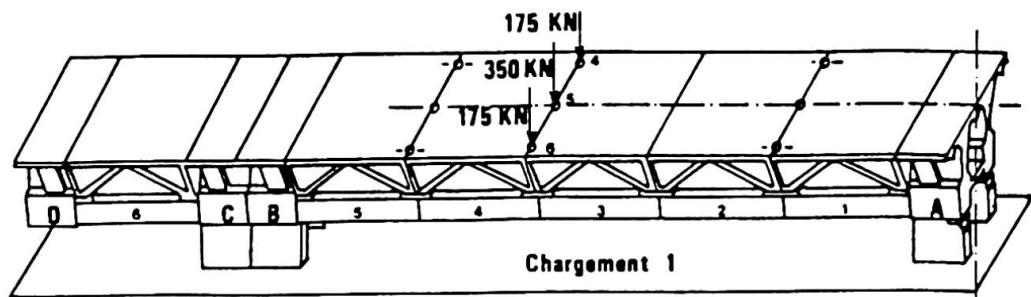
Toutefois, il faut noter que ces moments locaux dans les diagonales restent faibles (de l'ordre de 4 KNm) et se traduisent par des variations de contraintes dans la section inférieure à 2.5 MPa.

Dans le voussoir 1 (diagonales en béton armé), l'interprétation est plus difficile. En effet, la déformation enregistrée est très variable selon l'état de fissuration de la diagonale ; il peut même y avoir des écarts sensibles entre les jauges de 2 sections d'une même diagonale. En fait, on oscille entre deux extrêmes :

— une raideur correspondant à la section homogénéisée,

— une raideur correspondant aux armatures seules.

Il semble donc que l'on puisse admettre les hypothèses de calcul suivantes :

— diagonale comprimée : section homogénéisée,

— diagonale tendue : section des aciers seuls.

En effet, dans ces conditions, les modèles de calcul sont en accord avec les résultats expérimentaux ; on constate alors que l'assouplissement par la fissuration de la diagonale tendue entraîne un transfert plus important de l'effort tranchant vers les hourdis.

3 — CONCLUSION

3.1. Déformabilité de la structure

La déformabilité d'effort tranchant des structures treillis en béton ne peut-être négligée comme il est loisible de le faire dans les structures à âmes pleines.

Bien entendu, ces déformations supplémentaires accroissent les flèches de l'ouvrage, mais surtout, elles affectent la répartition des efforts dans les ouvrages hyperstatiques en diminuant les moments de flexion sur appui, et, en conséquence, en les augmentant en travée.
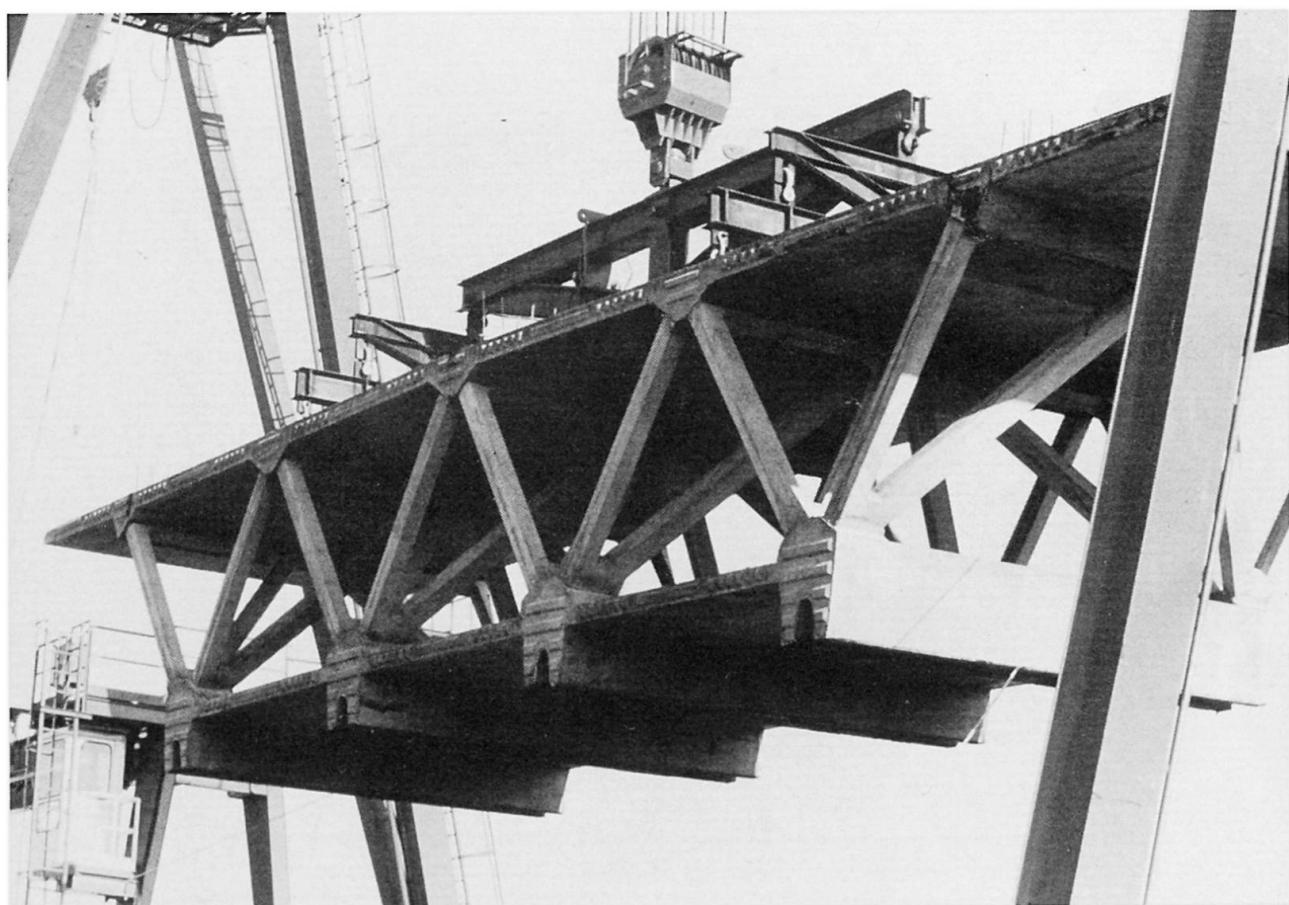
Figure 1 — Manutention d'un voussoir préfabriqué du pont de BUBIYAN

COMPARAISON DES RESULTATS EXPERIMENTAUX
ET DES RESULTATS DE CALCUL

DIAGONALES EN BETON ARME
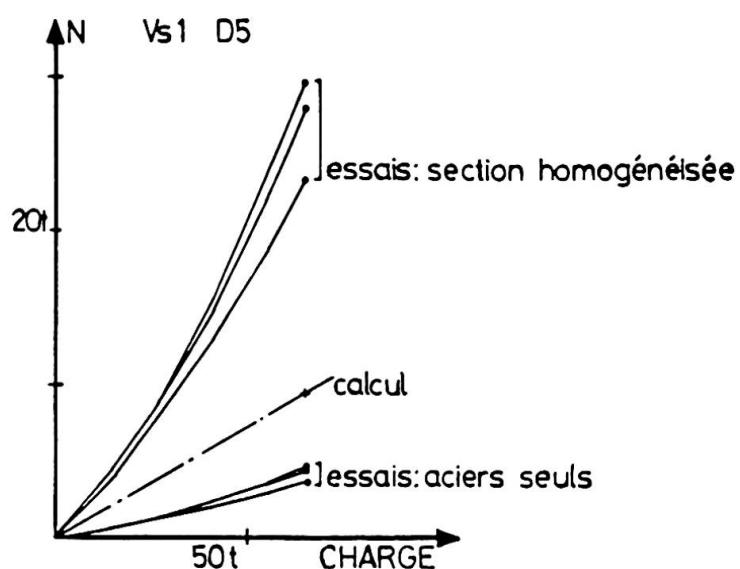
DIAGONALES PRECONTRAINTES
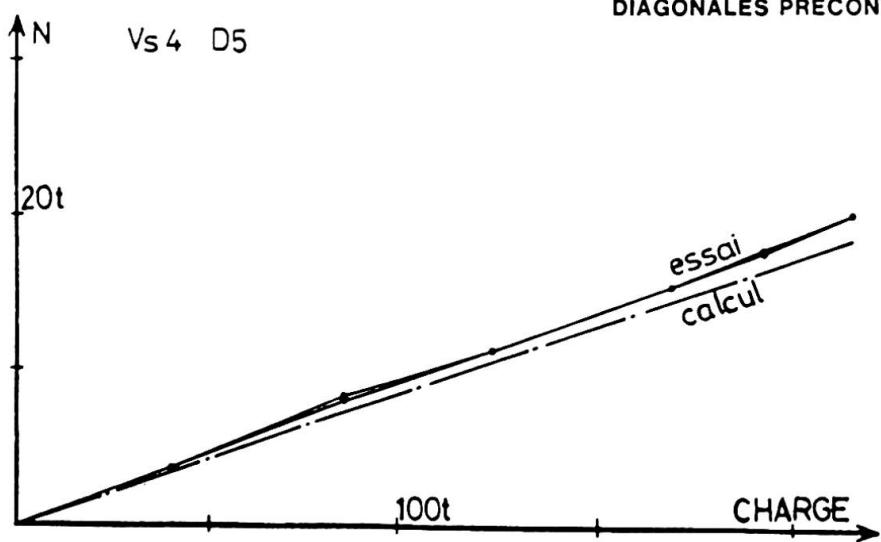
3.2. Modèles de calcul

— Lors d'études préliminaires, il est tout à fait possible d'étudier d'une part la flexion, reprise pour la poutre en I constituée des hourdis seuls, et d'autre part l'effort tranchant repris par la triangulation seule.

— Pour des études de détails, une excellente précision est obtenue en utilisant un modèle de calcul à barres, avec des sections homogénéisées pour les barres comprimées et des sections réduites aux aciers seuls pour les barres tendues.

3.3. Fonctionnement de la structure

D'une manière générale, le fonctionnement en phase de service est totalement satisfaisant.

En particulier, la linéarité des déformations au cours des diverses phases de chargement, ainsi que leur réversibilité ont été remarquables.

En outre, ce comportement est resté satisfaisant sous charges de service multipliées par 2.7.

En conséquence, il est possible de conclure que malgré la fissuration naturelle des diagonales en béton armé, cette structure conserve un comportement parfaitement élastique.

Dynamic Behaviour of Partially Prestressed Concrete Structures

Caractéristiques dynamiques des structures en béton partiellement précontraint

Dynamisches Verhalten von teilweise vorgespannten Betonbauwerken

Tiehan TANG
Bridge Engineer
Acad. of Railway Sciences
Beijing, China
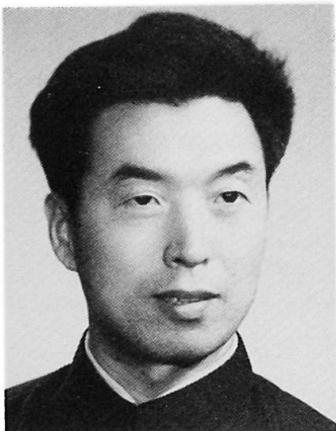
Tiehan Tang, born in 1938, graduated from the Tangshan Railway College, China, in 1963, completed post-graduate studies in 1966 under the direction of Prof. Lao Yuan-Chang. For over ten years he has been engaged in the design and research of bridge and building structures. His present research interest is partially prestressed concrete bridge structures.

SUMMARY

In order to study the dynamic behaviour of the tension zone in partially prestressed concrete structures a series of dynamic tests on axially tensioned specimens were conducted simulating the tension zone of beams. The tests demonstrated the dynamic effects on the stiffness of specimens, the relationship between the crack width and number of dynamic loading cycles, and the fatigue behaviour of both prestressing and nonprestressing reinforcements.

RESUME

Une série d'essais dynamiques de traction a été entreprise sur des éprouvettes afin d'étudier le comportement, dans les zones de traction, de structures en béton partiellement précontraint. Les essais ont montré les effets dynamiques sur la rigidité des éprouvettes, la relation entre la largeur des fissures et le nombre de cycles de charges et le comportement à la fatigue des armatures précontraintes et normales.

ZUSAMMENFASSUNG

Zur Erforschung des dynamischen Verhaltens der Zugzone von teilweise vorgespannten Bauteilen wurde eine Reihe von Versuchen an axial auf Zug belasteten Prüfkörpern durchgeführt. Die Belastung entsprach der Beanspruchung der Zugzone eines Biegeträgers. Die Versuche zeigten den Einfluss der dynamischen Belastung auf die Steifigkeit, das Verhalten der Risse in Funktion der Lastwechselzahl sowie das Ermüdungsverhalten des Vorspannstahls und des schlaffen Stahls.

1. INTRODUCTION

In PPC (partially prestressed concrete) structures under service loading, cracks are sometimes permissible in the concrete tension zone. Since cracks under dynamic loading show repeated progressing it is necessary, in order to achieve an appropriate evaluation of the service reliability of a structure, to carry out studies not only on its static behaviour, but also on the stiffness diminuation in its tension zone under dynamic loading, the dynamic effect upon crack development, and the fatigue behaviour of reinforcement as well. Hence a series of dynamic tests on axial-tension specimens were conducted simulating the reinforcement percentage in the effective area of tension zone of a beam subject to bending and reinforced with both prestressed and non-prestressed steels. The tests results rendered it possible: to establish the relationship between the tension zone stiffness of PPC structures and the dynamic effects; to investigate the relationship of the crack width versus the number of dynamic loading cycles and the reinforcement stress increase; to evaluate the fatigue life of both the prestressing and the non-prestressing reinforcements in the tension zone of structures provided with mixed reinforcement.

The tests showed that it is feasible to investigate dynamic effects on the tension zone in bending members through dynamic tests on axially loaded specimens.

2. TEST

2.1. Specimen and gauge points

Fig. 1 shows the configuration and dimensions of the specimen. 40 Si2MnV spiral bars were used for prestressing steel, with a diameter of 25 mm and an ultimate strength of 882.6 MPa. 20MnSi spiral bars 12 mm in diameter with an ultimate strength of 588.4 MPa were used for non-prestressing steel. The layout of the gauge points is also shown in Fig. 1. 10-inch (base) hand strain gauges were used to measure the following parameters: elastic compression of the specimen at the moment of tension-releasing; creep-shrinkage of the test specimen; strains in the specimen caused by static/dynamic loads. For the measurement of cracking load and decompressing load electric-resistance gauges were used.
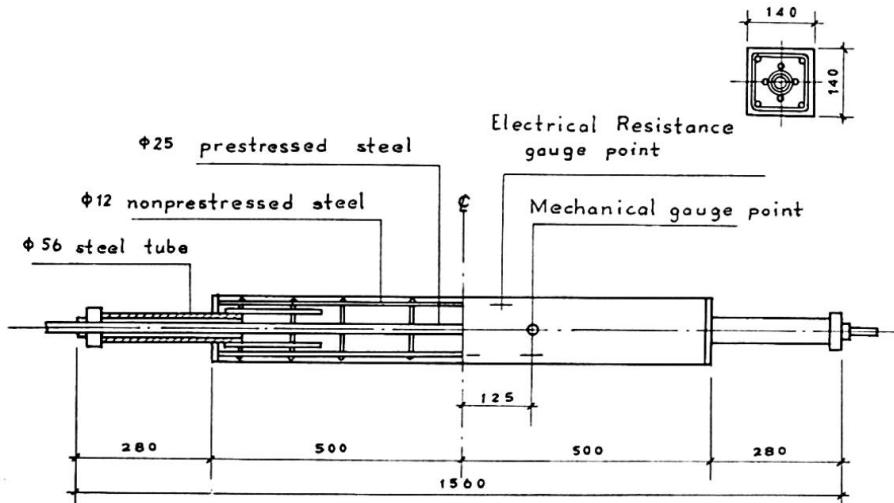

Fig. 1 Tensile specimens

2.2. Test procedures

Static test: aimed to determine the specimen stiffness in the elastic range and to measure its cracking and re-cracking loads. In each phase of dynamic load application (usually 5×10^5 cycles), static measurements were made to find out the dynamic effects on the stiffness and crack width of the members.

Dynamic test: Two different sets of tests were carried out. The first set was the dynamic crack-inducing test (A2-3(15)(17)), intended to help determine the dynamic load effect upon the cracking behaviour of the members subject to dynamic loading, the maximum value of which was kept under the cracking static load. It was also intended to enable observation of the entire process of variation of stiffness and crack width of the speciment with increasing dynamic loading cycles. The second set was the post-crack fatigue tests for determining the dynamic effects upon crack width and for measuring the ultimate fatigue strength of prestressing bars.

2.3 Load application

The load was applied to the specimen placed a fatigue testing machine through a special loading device which transformed the jacking pressure into a tensioning force applied to the specimen (Fig. 2). The magnitudes of the load were specified as follows:

(a) max. load $P_{max} < 156.9$ kN for the static elastic loading phase;

(b) $P_{min} < P_d < P_{max}$;

(c) $\sigma_{p,max} / \sigma_{pu} = 0.5 - 0.6$ for the upper limit of the dynamic load;

(d) the minimum load to be so chosen in correspondence with the prescribed maximum load as to keep the ratio $\sigma_{p,min} / \sigma_{p,max}$ in the prestressing bars at around 0.7.

where P_{min} is the minimum load, P_d is the decompressing load of the members, P_{max} is the maximum load, $\sigma_{p,min}$ is

Fig. 2 Test equipment

the minimum stress of prestressing bars, $\sigma_{p,max}$ is the maximum stress of prestressing bars, σ_{pu} is the ultimate strength of prestressing bars.

3. DYNAMIC EFFECTS ON STIFFNESS OF SPECIMENS

Through dynamic tests made on specimens A2-3(15) and A2-3(17) using hand strain gauges for step-by-step measurement in accordance with the loading sequence, the variation of the specimen stiffness with the increase of the load was well as the number of load applications was found out. In Table 1 are given the loading procedure and the corresponding stress values in the prestressing bars.

The range of the hand strain gauge was 10 inches, covering three cracks.

The measurements gave the average strain in this section, showing the bond deteriorating between concrete and steel and the influence of concrete stiffness dwindling as a consequence of the increase in the number of dynamic load applications. In Fig. 3 are shown the variation curves of the measured average strain values.

Loading sequence	1		2		3		4		5		6	
Load (kN)	max	min	max	min	max	min	max	min	max	min	max	min
	176.5	70.6	196.1	78.5	215.7	86.3	235.4	94.1	255.0	102.0	274.6	109.8
$\sigma_p.max$(MPa)	472	367	495	368	519	370	543	374	574	392	589	393
$\Delta\sigma_p$ (MPa)	105		127		149		169		182		196	
N ($\times 10^4$)	$4 \times 50 = 200$		66		50		50		50		50	

Table 1 Load, stress and cycles for specimen A2-3(15)
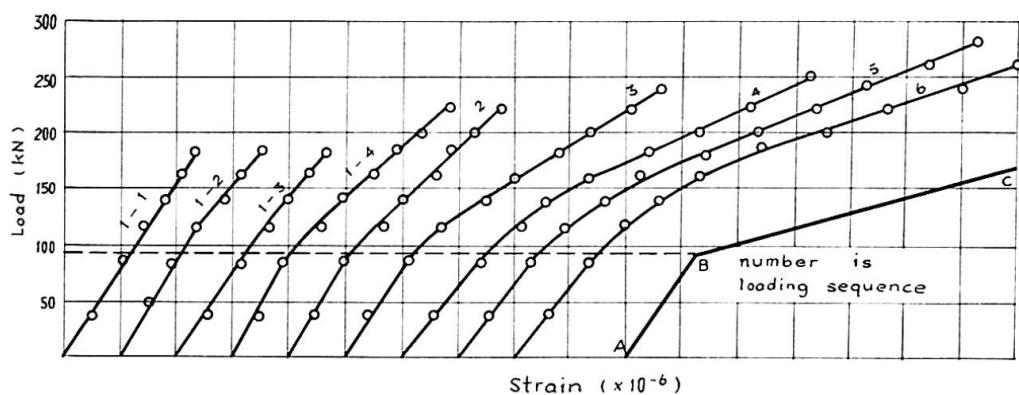
Fig. 3 Loading cycles vs strain for specimen A2-3(15)

The first sloping line at the left hand of the figure represents the load/ strain curve for the first load application. It can be seen without difficulty that the specimen in this case is in the range of linear elasticity before the appearance of cracks. All the other curves are load/strain ones obtained from measurements made according to the loading sequence. The curves deflect downward in their upper portions as the number of loading cycles and the load magnitude increase until the loading cycle reaches around 4×10^6 when the up-per portion becomes nearly parallel to the curve section BC (drawn in bold line) at the right hand of the figure. This BC line is the load/strain curve for the measured section when the external load is considered to be taken up by the prestressing and non-prestressing steels only. Apparently, the effect of concrete stiffness in this instance is completely null. The broken line ABC is an idealized load/strain curve for 4×10^6 cycles of repeated load application.

Some preliminary conclusions can be drawn from the above test results:

(1) For the first 5×10^5 loading cycles, the upper limit of the dynamic

load equals the maximum static load on first application (without appearance of any cracks), P_{max} = 176.5 kN. However the load/strain curve exhibits marked deflection for P >88.3 kN. This implies that the specimen has been dynamically loaded to crack. With continued application of load up to 2 x 10^6 cycles, the upper limit remaining unchanged, the slope of the deflected section of the load/strain curve does not show any noticeable change but the point of deflection moves downward slightly. This demonstrates that the number of cycles bears no significant influence on the specimen stiffness for lower levels of dynamic loading, even though cracking has heretofore occurred.

(2) As obtained from measurement, the average value of the re-cracking load (decompressing load) of the specimen is P_d = 91.7 kN. It is observed from Fig. 3 that, with the accumulation of loading cycles, the upper portion of the load/strain curve slopes further downward, yet the lower portion of the curve maintains basically the same inclination as that of the original linear elastic curve (the first curve at the left hand of the figure). This indicates that the cracked specimen will close up and resume its elastic behaviour under the action of prestressing force on the removal of the dynamic load which is not very large. Beyond the point where the upper limit of the dynamic load exceeds 235.4 kN, the upper portion of the curve is practically parallel to line BC with the concrete entirely out of function. In this case, the curve cannot regain its original slope on unloading to 88.3 kN and under, when the stress in the prestressing bar would have increased by 166.7MPa, which is highly improbable to occur under normal service loading conditions.

4. DYNAMIC EFFECT ON CRACK WIDTH

As has been described in the foregoing paragraphs, the bond between the tension reinforcement and the concrete in PPC structures deteriorates gradually under the action of dynamic loads, and the concrete gradually recedes from its function. At the same time, the crack width in the concrete tension zone also displays some changes.

In this test 13 specimens were put under dynamic loading and were observed for the development of crack widths. For this purpose systematic observations and measurements were made on specimens A2-3(2)(11)(16)(20)(21). The measured static cracking loads and decompressing loads for the 5 specimens before they were put under dynamic test are given in Table 2. The corresponding crack widths measured under different loadings are summed up in Fig. 4. Regression analysis of the measured data gave the following relationship: w = -0.0534 + 0.00693 P. From this can be obtaned the calculated decompressing load P_d = 75.5 kN at w = 0. This calculated value is slightly smaller than the average value given in Table 2.

Transforming the above regression equation into the correlation equation of crack width against stress increase in prestressing steel, we have:

$$w = 0.57 \, \Delta\sigma \times 10^{-3} \text{ (mm)}$$

where $\Delta\sigma$ is the stress increase in the prestressing steel in MPa.

Specimens Load (kN)	A2-3(2)	A2-3(11)	A2-3(16)	A2-3(20)	A2-3(21)	Average
Crack Load P_{cr}	124.5	160.8	192.2	165.2	140.7	156.8
Decompresing Load P_d	73.5	81.4	96.1	70.1	74.5	79.1

Table 2 Cracking and decompressing loads

5. FATIGUE BEHAVIOUR OF SPECIMEN

Studies of the fatigue behaviour of PC structures are generally carried out on
real members or model beams. Sometimes such a study is done with prestressing
steel and concrete separately. The first method involves expensive costs, and
the test is limited in scale, while with the second method the applicability
of the test results to fatigue design of actual structures is yet to be exami-
ned. In this paper, another method of fatigue test is described. This method
reveals the fatigue behaviour of the tension zone of a bending members with
united action of concrete, prestressing steel and non-prestressing steel in
carrying the dynamic load. And it is simple, explicit and inexpensive.
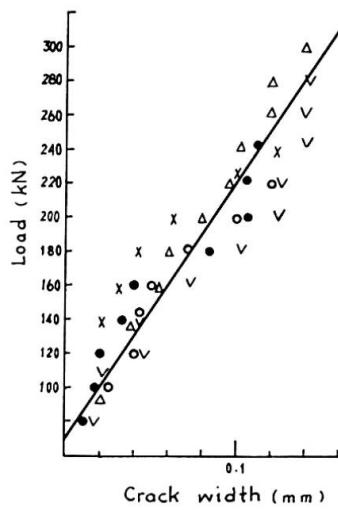
Fig. 4 Crack width
        vs load
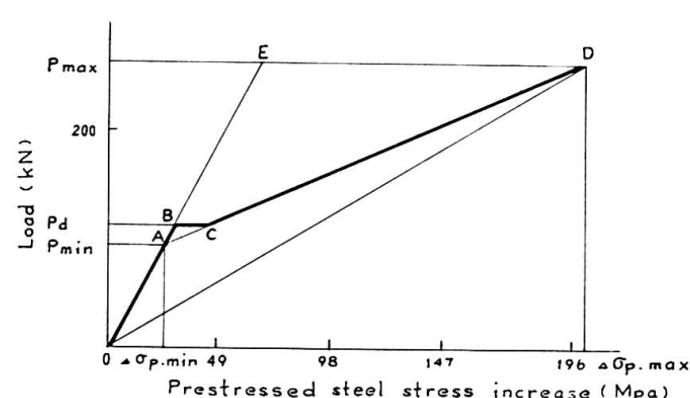
Fig. 5 Prestressed steel stress
        increase vs Load

The loading procedure for the fatigue test was the same as described in para-
graph 2. The fact that the range of fatigue test load defined by its upper
and lower limits contained the decompressing load for the specimen reflects
the most unfavourable condition for fatigue resistance of the tensionzone of
PPC structures. Fig. 5 shows the theoretical correlation curve of the load
versus the stress increase of the prestressing steel for specimen A2-3(12).
The sloping line OE in the figure is equivalent to the correlation curve for

full prestressing. Since generally $P_{min} < P_d < P_{max}$ (in the case of bending member $M_{min} < M_d < M_{max}$) for PPC structures, the stress increase in prestressing steel will vary along the curve definid by 0, B, C and D. This curve, being a theoretical one with its BC section a smooth line, has been verified by test results. It can be seen from Fig. 5 that, in the case of PPC structures subject to dynamic loading, there is an abrupt change of stress increase in the steel at the crack. Thus for the same load amplitude the stress increase becomes larger than that in the case of fully prestressed concrete structures.

In Fig. 6 are summed up the results obtained form the fatigue rupture tests of 11 specimens. In all cases, the break point was located in the effective middle portion of the specimen. Regression analysis gave the equation of correlation between the cycle number N and the stress behaviour of the prestressing steel S_{max}.

$$S_{max} = 1.265 - 0.1105 \text{ Log } N$$

where $S_{max} = \sigma_{p,max} / \sigma_{pu}$, where $\sigma_{p,max}$ being the maximum prestressing steel stress value at the point of fatigue rupture, σ_{pu} the ultimate strength of the prestressing steel with an assumed value of 944 MPa.

Given the correlation factor r = -0.8316 and remnant standard difference S_x = 0.245, the fatigue strength of prestressing steel corresponding to 2×10^6 cycles was calculated as follows: $S_{max} = \sigma_{p,max} / \sigma_{pu} = 0.5774$, $\sigma_{p,max}$ = 546 MPa. Assuming 95% as the guaranctee rate, the average value of fatigue strength $\sigma_{p,max}$ = 513 MPa, $\sigma_{p,min}$ = 341 MPa, $\Delta\sigma$ = 172 MPa.

As has been demonstrated by tests, the PPC structures with mixed reinforcement as described in this paper can satisfy service requirements under dynamic loading so far as fatigue life is taken into consideration.

It was found on cutting the specimens across through the fatigue break point that in all cases fatigue break occurred on prestressing steels, shown in Fig. 7, whereas all non-prestressing steels were still in good order. Computational analysis also indicated that it was only natural for the prestressing steel, the maximum stress amplitude of which under dynamic loading had reached 196 MPa, to fail by fatigue prior to non-prestressing steel, which had an initial compression due to its constraining effect against concrete shrinkage and creep, and thus had a stress amplitude as low as 78 MPa.
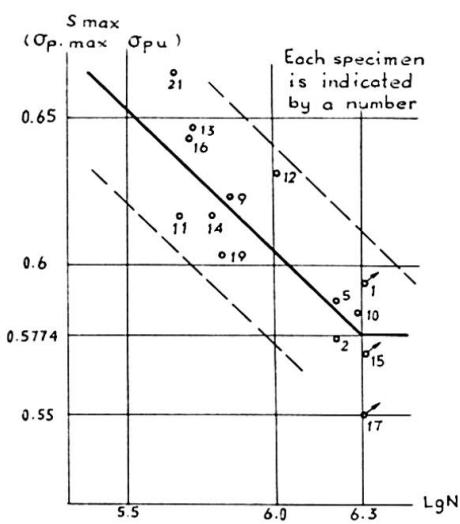
Fig. 6   S-N curve for prestressing steel
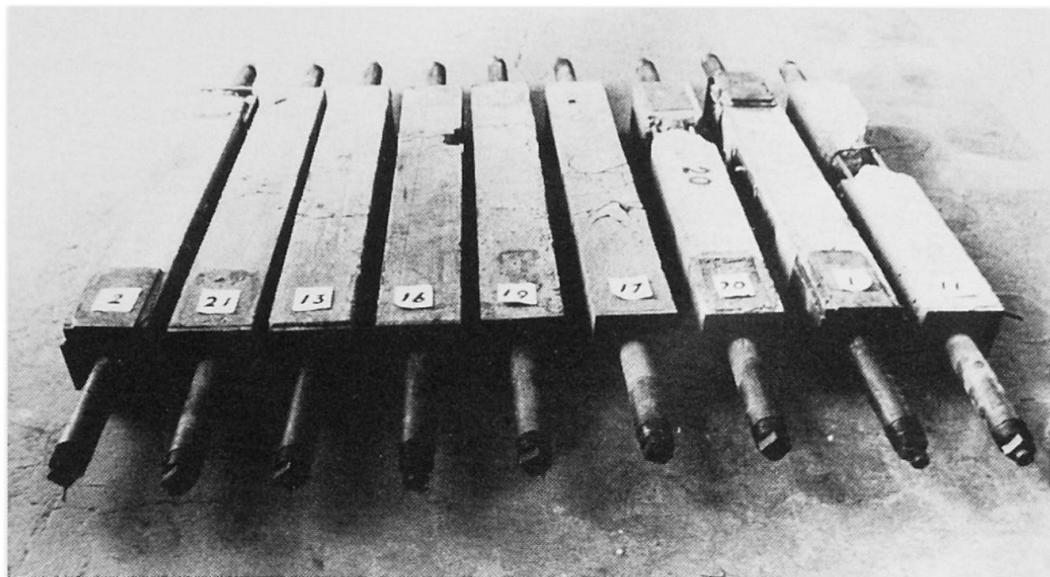
Fig. 7   Specimens after break

The hereby adopted method of experimental study may be applied to structures using forms of reinforcement other than mentioned in this paper. Its practical significance will be further manifested when the test results are compared with those to be obtained from bending beams using the same form of reinforcement.

ACKNOWLEDGEMENTS

Eccentrically Loaded Concrete Columns; 15 Years of Sustained Load

Poteaux de béton sous charges excentriques; 15 années de charge soutenue

Exzentrisch belastete Stützen; 15 Jahre Dauerbelastung

R. GREEN
Prof.
Univ. of Waterloo
Waterloo, ON, Canada

Author of papers on columns, bridge vibration and steel construction. Member of the Code Development Committee of OHBDC and Committee CSA A23.3.

John E. BREEN
Prof.
Univ. of Texas
Austin, TX, USA
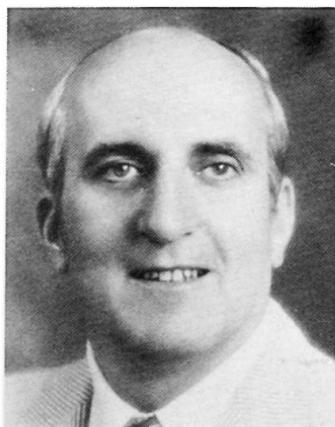
Director of the Phil M. Ferguson Structural Eng. Lab. at Austin. Author of papers on reinforced and prestressed concrete research and development. A former Chairman of ACI TAC and the new Chairman of Committee ACI 318.

SUMMARY

The sustained load response of ten unrestrained eccentrically loaded columns is described for an observation period of 15 years. Results of observations are compared with values given by the ACI 318-83 code. Analyses incorporating the time dependent characteristics of concrete permitted the prediction of failure times, deflections, and capacities to acceptable accuracies.

RESUME

Le comportement de poteaux non-encastrés, soumis à des charges continues et excentriques pour une période de 15 ans, est décrit. Les valeurs mesurées sont comparées à celles de la norme ACI 318-83. Des analyses incorporant les caractéristiques du béton en fonction du temps permettent de prédire les temps de rupture, les déformations et les résistances selon les limites permises.

ZUSAMMENFASSUNG

Das Verhalten von zehn seitlich ungehaltenen, exzentrisch belasteten Stützen unter Dauerlast wird beschrieben. Die Beobachtungsperiode betrug 15 Jahre. Die Versuchsergebnisse werden mit den Werten der Norm ACI 318-83 verglichen. Eine analytische Berechnungsmethode, die die zeitabhängigen Charakteristiken des Beton berücksichtigt, erlaubt die Bestimmung der Standzeit bis zum Bruch, der Verformungen wie auch des erforderlichen Widerstandes für eine bestimmte Standzeit und Last.

1. INTRODUCTION

The analysis of reinforced concrete columns under sustained load can be difficult and time consuming. Data describing the effects of various sources of material nonlinearity must be combined with member geometric nonlinearity if the load-deformation-time response of slender compression members is to be predicted.

In the mid 1960's, when these studies of eccentrically loaded slender columns under sustained load began [1] most previous studies had been concerned with the sustained load behavior of axially loaded columns or with the maximum sustained load capacity of short eccentrically loaded columns. Some results pertaining to sustained load responses of slender columns ($\lambda \simeq 100$) were also available [2]. The studies of the 1960's were intended to provide a more general approach covering not only the overall response of a column to sustained load, but also the load-moment-curvature-time sectional behavior. Based on this behavior, it was expected that the time-dependent-stress-strain model would allow the prediction of sectional response, and member response.

In this paper, tests over a duration of 15 years on a series of ten unrestrained eccentrically loaded columns are described. The results include columns which crept to rupture and others which were still stable following nearly 15 years of sustained load. The stable columns were loaded to failure in a short time without unloading. The response of columns to load is predicted using a simple analysis and also a more complex analysis where the history of loading of individual concrete fibers is considered. It was possible to predict the load-deflection-time characteristics of concrete columns with complex loading histories.

2. THE TEST, THE SPECIMENS AND THE PROCEDURE

2.1 The Test

The histories of specimen loading are illustrated in Figure 1. Upon loading, deflections are present along the length of the column (Figure 1a). These deflections increase due to creep of the concrete in the column, thereby increasing the moments throughout the column length under sustained load.

Two possible loading histories are illustrated in Figures 1b and 1c for the column of Figure 1a. One history has creep buckling occurring at some time t_f under a sustained load, N_s (Figure 1b). The second is the failure at load N_f
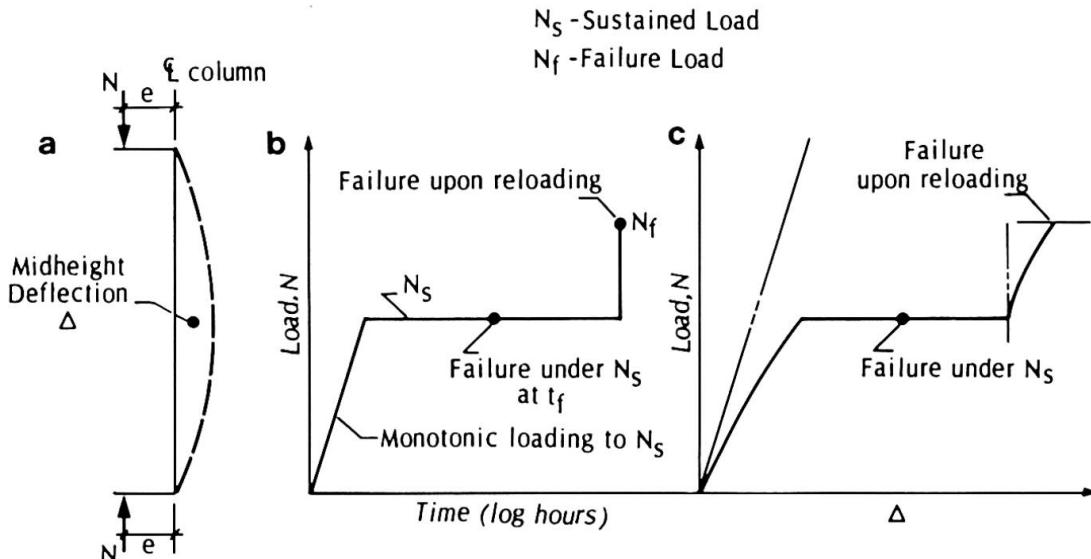
Fig. 1 Load Histories

developed due to further loading after a sustained load duration, t (Figure 1c). Data from columns having both loading histories obtained in the test series.

2.2 The Specimens

The specimens had a nominal cross section of 100 mm by 150 mm, a slenderness ratio (λ) of approximately 63, a reinforcement ratio (ρ) of 0.02, an average concrete cylinder strength of 28 MPa at the time of initial loading and an average reinforcing steel yield point of 420 MPa. Details of the specimen section are given in Figure 2.

A controlled environment was not available which would accommodate the ten specimens and associated equipment. A calculated risk was taken that the test house environment would correspond to that found near full size structural elements. The average temperature and relative humidity recorded at the test location over a 2 year period were 22°C and 65% respectively, with ranges of approximately 0°C to 35°C, and 35% to 95% respectively.

2.3 The Procedure

The loading system and instrumentation permitted the following:
- application of axial load, N, at a predetermined end eccentricity, e.
- measurement of axial load.
- maintenance of a sustained axial load to within approximately +3% and −5% of the desired value over the 14.5 year test period.
- test to failure without unloading the column.
- measurement of average curvature at various sections along the column length.
- deflections at several points along the column.
Full details of the test procedure are available [3] and an overall view of the test house is given in Figure 3.

Loads were applied through load cells and sustained using two 1/2 in. diameter prestressing strands linked to heavy duty coil springs. Columns were tested in a vertical position with the average age at initial loading of 49 days. Creep and shrinkage studies were carried out.
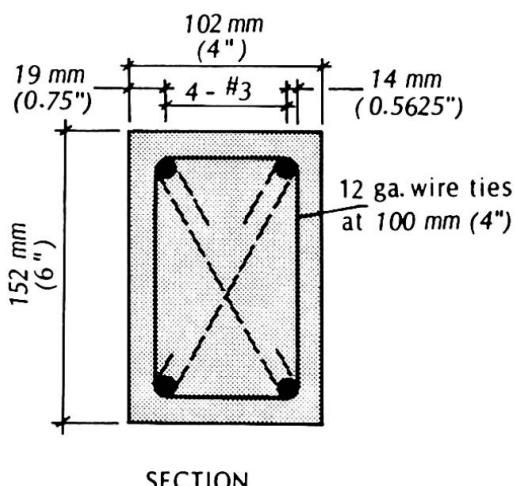
Fig. 2 Cross Section
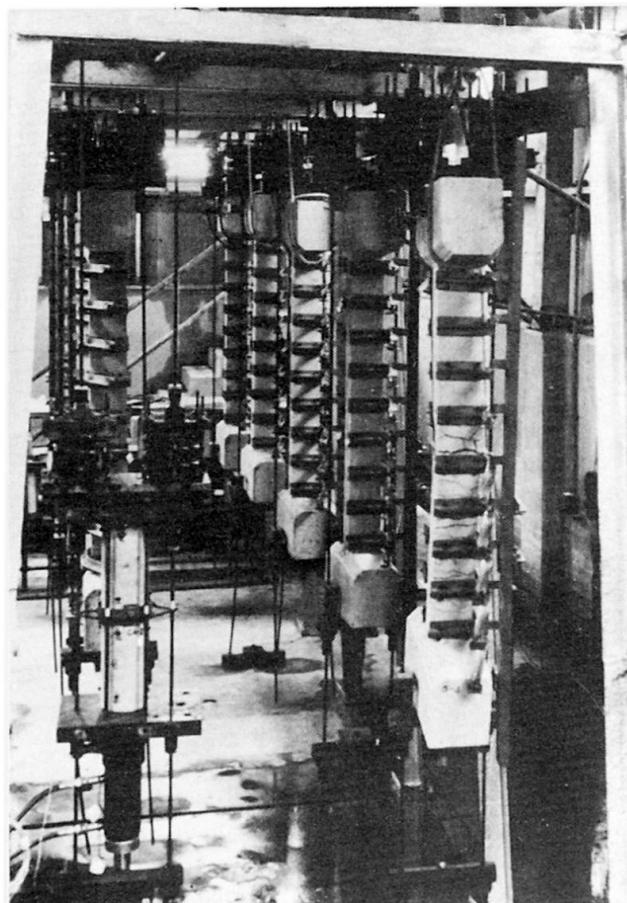
Fig. 3 Test House

3. THE TEST RESULTS

In the absence of more detailed criteria, sustained load levels were chosen such that the calculated service (specified) axial load capacities of the columns based on ACI 318-63 [4] were exceeded. The ratio of sustained to service load ranged from 0.98 to 1.97. Service load capacities were calculated using the R-factor method of ACI 318-63, a capacity reduction factor of 1.0 and equal specified dead and live loads. Subsequent references to loads and capacities are not based on ACI 318-63, the Code available at the beginning of testing, but rather the most recent edition of ACI 318, published in 1983 [5]. Values of sustained load, failure load, failure time, and capacity ratios based on ACI 318, are given in Table 1 for the columns. Table 2 provides N_s/N_o values, N_s/N_c values and associated e/h values for all columns. Examination of Tables 1 and 2 indicates:
- good coverage in terms of N_s/N_o (0.18 to 0.47) and e/h (0.04 to 0.42) for a typical interaction diagram [1].
- ratios of sustained load to ACI 318 capacities varying from 0.90 to 1.40.
- sustained load failure of specimens having a $\bar{N}_s$ ratio greater than 1.20.
- failure load capacities, $\bar{N}_f$, subsequent to sustained loading in excess of 1.20 $\bar{N}_s$ for those columns still stable after 14.5 years under sustained load.

3.1 Typical Results

The load-midheight (maximum) moment results for two typical columns are given in Figure 4, together with an interaction diagram based on the cylinder strength of the concrete at initial loading. Column S1 failed due to creep instability following approximately 7.7 years of sustained load, which was in excess of the ACI 318-83 capacity. Column S7 failed due to instability, when reloaded after 14.5 years of sustained load, but at a load level in excess of the original short-time capacity predicted using ACI 318-83. The initial midspan deflections

Specimen	Sustained Load, N_s, kN	Failure Load, N_f kN	Time at Failure t_f	Capacity Ratio[*] $\bar{N}_s$	$\bar{N}_f$
S1	236	236	7.7 yrs	1.39	---
S2	121	176	14.0 yrs	0.92	1.33
S3	189	252[+]	14.0 yrs	0.92	1.23
S4	187	187	74 h	1.42	---
S5	185	185	4.9 yrs	1.19	---
S6	162	162	1037 h	1.22	---
S7	129	229	14.2 yrs	0.95	1.70
S8	133	167	14.4 yrs	1.09	1.37
S9	134	134	1 h	1.41	---
S10	80	102	14.5 yrs	0.95	1.20

[+]Loaded to failure at 252 kN by increasing end moment

[*]Capacity ratio $\bar{N}_s$ or $\bar{N}_f$, Ratio of N_s or N_f, if reloaded, to calculated capacity, N_u, using ACI 318-83, $\beta_d = 1.0$, $\phi = 1.0$.

Table 1

Number of Specimens	N_s/N_o	e/h	N_s/N_c
1	0.47	0.04	0.22
3	0.36 to 0.38	0.11, 0.16, 0.18	≈ 0.16
4	0.26 to 0.29	0.04, 0.15, 0.27, 0.42	≈ 0.12
2	0.18, 0.19	0.25, 0.42	≈ 0.085

Table 2
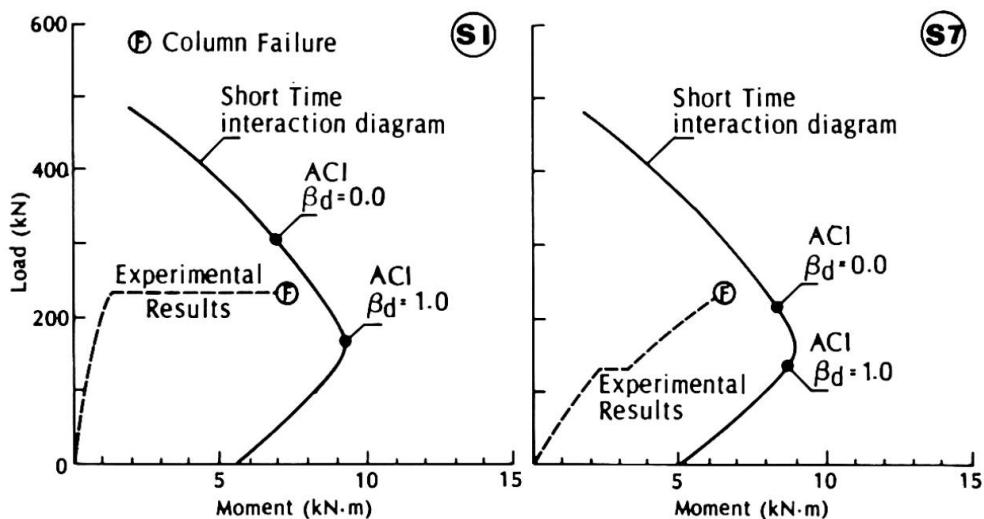
Fig. 4 Load Moment Values, Columns S1 and S7
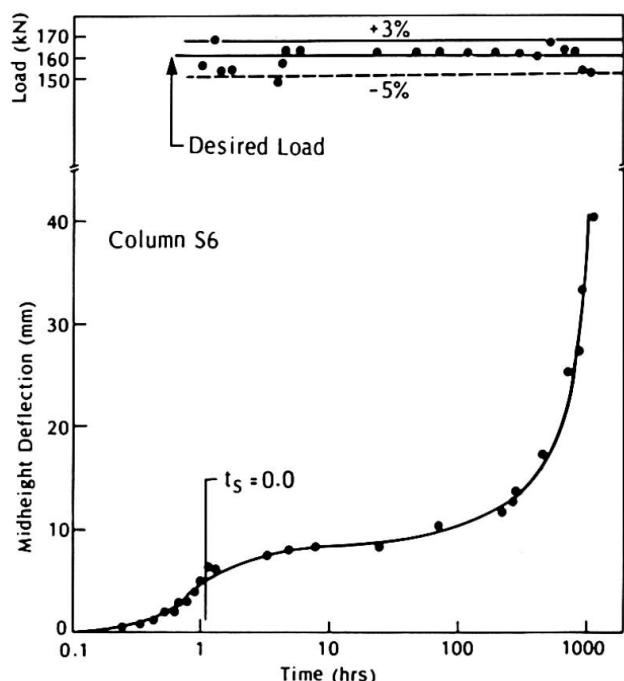
Fig. 5 Data, Column S6

for Column S1 increased by more than 15 times prior to failure. Deflections increased four-fold for Column S7.

Deflection-time data obtained from Columns S6 and S7 are given in Figures 5 and 6. Deflection increased rapidly as creep instability occurred (Column S6). Reference to the curvature meter data and associated surface strains indicated average strains on the "compression" face of Column S6 of 0.007 at approximately 1000 h. Powdering of the concrete on the compression face was observed just prior to failure. Also shown as part of Figure 6 are load-time data indicating load adjustment following creep shortening of the column. Some loss of sustained load occurred near failure. A gradual increase in deflection with time was found for Column S7 (Figure 7).
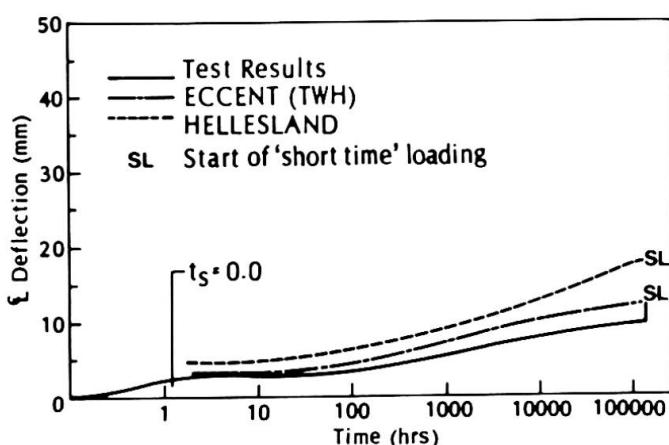
Fig. 6   Data, Column S7

The load-deflection data (Figure 7) illustrates an interesting feature of column response following sustained load.   The initial portion of the load-deflection curve is slightly nonlinear as a consequence of secondary bending.   Creep increases deflection with time.   Upon reloading, there is

Fig. 7 Load-Deflection Values

an appreciable increase in the tangent stiffness value for the column.   There was little warning before member failure and ductility appeared limited.

3.2 Material Characteristics

Companion creep tests carried out using 150 mm times 300 mm cylinders indicated a creep coefficient of 4.0 at 14 years.   A shrinkage strain of approximately 200×10^{-6} at 14 years was observed.   Cylinders cast and stored in the test house with the specimens, and then tested at 14.5 years had an average strength gain of 0.2 times the initial compressive strength.

4. ANALYSIS

An initial objective of the study [1] was to establish a simple and reasonably accurate model of column section behavior for the prediction of member response to short-time loading, sustained loading and short-time loading following sustained load.   The model was to consider the accepted physical characteristics of concrete.   Similar models applicable to uncracked reinforced or prestressed concrete members with low stress intensities have been developed recently [6].

4.1 Material and Section Model

Moment-curvature-time data (not shown) [1,3] obtained during the initial 0.6 years of the study were used to develop time-dependent-stress-strain (tdss) curves with the following characteristics:
- a parabolic form up to a maximum resistance of 0.95 f'_c at ε_o (≈ 0.002) and a descending branch, for short-time loading.
- a reduction in maximum resistance to 0.75 f'_c due to long-term sustained stress.
- a bilinear creep function applied to the short time stress-strain curve, based on Reference [7].
- a creep coefficient of 4.2 at 14 years.

Fig. 8 TDSS Curves

Fig. 9 M-φh-t Curves

Analysing the full 15 year data set, Traynor included hardening using a linear log time function for continued concrete hydration in predicting short-time concrete response subsequent to sustained loading [8]. A series of tdss curves (Figure 8) were developed to create a corresponding set of moment-curvature curves for a known section corresponding to a desired loading history (Figure 9). The moment-curvature data form input to a member analysis routine, Newmark's Method [9] in this case. For reloading after t_s, the deformed configuration due to sustained load was taken as an initial imperfection in the short time reloading analysis. Traynor developed the computer code ECCENT (TWH) for member analysis. The results obtained are identified in Figures 6 and 7 by the code name.

4.2 Member Model

Member responses were obtained from a quasi-static, single point collocation propagation analysis due to Hellesland [10]. The model of the concrete fiber behavior includes creep, shrinkage, strength loss and hydration effects. Use of the model requires data about concrete strength, creep coefficient and shrinkage as well as member geometry. A uniform sectional behavior is assumed throughout the member.

4.3 Comparisons

Both the ECCENT (THW) and Hellesland analyses predict behavior satisfactorily (Figures 6 and 7). In Figure 7, ECCENT (TWH) underestimates the deflection at the end of sustained loading period for Column S2 while the converse is true for Column S7. Failure loads are predicted well and the hardening after sustained load is reflected by the analysis. The Hellesland Model predicts failure loads but underestimates the stiffness upon reloading (Figure 7). The rapid increase in midheight deflection under sustained load as failure approaches can be modelled using both analyses. However, predictions of failure time are difficult because of the
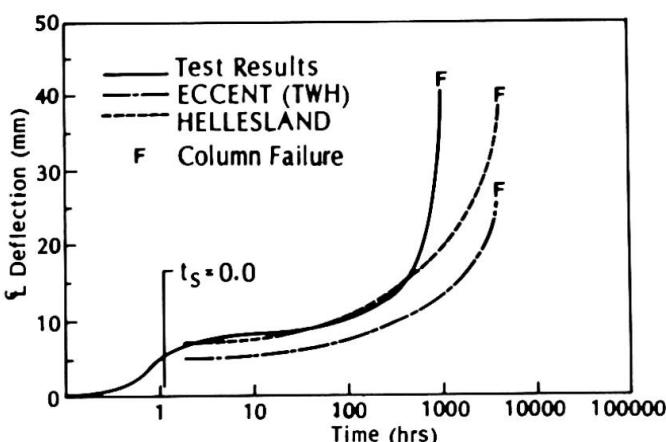
Fig. 10 Deflection-Time Results

uncertainty associated with prediction of concrete properties and short- and long-term deflections (Figure 10).

The following ratios were calculated in terms of observed to calculated values:
- failure times(logarithmic scale) ranged from 0.80 to 1.15 for both analyses.
- deflections including short-time and sustained loading, and reloading were between 0.8 and 1.6 at 14 years using the ECCENT (THW) analysis. (The Hellesland analysis tended to overestimate deflections upon reloading).
- ultimate capacities upon loading after sustained loading were 0.95 to 1.25 from both analyses.
- the ranges of the ratios quoted above are not unlike the deviations associated with the short-time behavior prediction of columns [11].

5. CONCLUSIONS

The results obtained indicate that it is possible to apply time-dependent-stress -strain curves to predict the response of eccentrically loaded columns to complex loading histories, if the creep coefficient and strength of the column concrete can be established. Such curves are easily applied in design practice. The test results provide confidence in the current calculation procedures advocated in ACI 318-83 for column strength under sustained load.

6. ACKNOWLEDGEMENTS

7. NOTATION

e - eccentricity with respect to centroid, f'_c - concrete cylinder strength h - overall length of column, N_c - elastic critical load based on gross transformed section short time, N_f - axial load resulting in failure, $\bar{N}_f$ - see Table 1, N_s - sustained axial load, $\bar{N}_s$ - see Table 1, N_o = axial load capacity at zero eccentricity $\phi = 1.0$, t_f - time of failure, t_s - time under sustained load, ε_o - strain at maximum fiber stress, λ - slenderness ratio.

REFERENCES

1. GREEN, R., BREEN, John E., Eccentrically Loaded Concrete Columns Under Sustained Load. ACI Journal, Vol. 66, No. 11, Nov. 1969.
2. GAEDE, K., Knicken von Stahlbetonstaben unter Kurz-und Langzeitbelastung. Bulletin No. 129, Deutscher Ausschuss für Stahlbeton, 1958.
3. GREEN, R., Behavior of Unrestrained Reinforced Concrete Columns Under Sustained Load. Ph.D. Dissertation, U. of Texas, Austin, Texas, 1966.
4. ACI Committee 318, Building Code Requirements for Reinforced Concrete (ACI 318-63). American Concrete Institute, Detroit, 1963.
5. ACI Committee 318, Building Code Requirements for Reinforced Concrete (ACI 318-83). American Concrete Institute, Detroit, 1983.
6. DILGER, Walter H., Creep Analysis of Prestressed Concrete Structures Using Creep Transformed Section Properties. PCI Journal, Vol. 27, No. 1, 1982.
7. RÜSCH, H., Researches Towards a General Flexural Theory for Structural Concrete, ACI Journal, Vol. 57, No. 1, July 1960.
8. TRAYNOR, L., Sustained Load Behaviour of Unrestrained Reinforced Concrete Columns. M.A.Sc. Thesis, U. of Waterloo, Waterloo, Ontario, Canada, 1984.
9. NEWMARK, N.M., Numerical Procedure for Computing Deflections, Moments and Buckling Loads. ASCE Transactions, Vol. 108, 1943.
10. HELLESLAND, J., A Study into the Sustained and Cyclic Load Behaviour of Reinforced Concrete Columns. Ph.D. Dissertation, U. of Waterloo, 1970.
11. Stabiliteit, Report 77, CUR, The Netherlands, 1976.

Reinforcement Strains in Reinforced Concrete Tension Members

Allongement de l'acier d'armature dans des tirants

Stahldehnungen in Zuggliedern aus Stahlbeton

R.H. SCOTT
Lecturer
University of Durham
Durham, England

Mr. Scott graduated from the University of London in 1968, and then spent ten years with a Consultant and Local Authority. He joined the Department of Engineering at the University of Durham in 1978 as a lecturer with special interests in concrete structures.

P.A.T. GILL
Senior Lecturer
University of Durham
Durham, England

Dr. Gill has degrees in mechanical engineering from Nottingham and Southampton Universities. He worked in the aero engine industry before joining Durham University in 1967. His principal interests are stress analysis and dynamics.

SUMMARY

This paper describes the technique which has been developed to measure longitudinal reinforcement strains in reinforced concrete tension members. A programme of short-term tests has been completed to date. The testing procedure is described and preliminary results presented.

RESUME

Cette contribution décrit les techniques développées pour mesurer les allongements relatifs de l'acier d'armature dans des tirants en béton armé. Un programme d'essais de courte durée a été réalisé. Le procédé d'essais et les premiers résultats sont présentés.

ZUSAMMENFASSUNG

Der Beitrag beschreibt eine eigensentwickelte Technik der Dehnungsmessung in der Längsbewehrung von Zuggliedern aus Stahlbeton. Eine Serie von Kurzzeitversuchen ist bis heute durchgeführt worden. Die Versuchsdurchführung wird beschrieben und die ersten Ergebnisse werden vorgestellt.

1.   INTRODUCTION

Calculation of the deflection of reinforced concrete structures requires an accurate assessment of the stiffnesses of the constituent members. With beams, in particular this is influenced considerably by the behaviour of the concrete in tension below the neutral axis.

Previous experimental work in this field has involved surface strain measurements on beams or tension specimens tested in the laboratory. The authors believed that useful further advances would result from a detailed study of the reinforcement strains themselves, particularly as modern strain measuring technology and data acquisition systems would permit this to be undertaken in a far more detailed manner than had been attempted previously [1, 2].

This is being achieved through a series of tests on tension specimens using internally strain-gauged reinforcing rods. Three series of tests are being undertaken covering short-term incremental, long-term sustained and long-term cyclic loadings. The short-term testing programme is now complete and long-term sustained load tests are currently in progress. Cyclic loading tests will commence later this year.

This paper describes the strain-gauging technique which has been developed to measure the longitudinal reinforcement strains. Details of the testing procedure and preliminary results for the short-term tests are presented.

2.   MEASUREMENT OF LONGITUDINAL REINFORCEMENT STRAINS

A prime consideration when selecting a technique for measuring reinforcement strains is to avoid altering the bond characteristic through degradation of the steel/ concrete interface. This effectively precludes bonding electric resistance strain gauges to the surface of the rod since the gauges and their associated lead wires disturb the stress fields around the reinforcement and the concrete. Consequently a solution was sought which would involve mounting strain gauges inside the reinforcement and thus leave the interface undisturbed.

The technique which was tried out and subsequently adopted involved milling two reinforcing rods down to a half round and then machining a longitudinal groove in each to accommodate the strain gauges and their wiring. After installation of the gauges the two halves were then glued together so that outwardly they had the appearance of a normal reinforcing rod, but with the lead wires coming out at the ends.

Early results using comparatively short rods were extremely promising [3] and have led to the development of the technique to the stage where eighty four strain gauges, each connected with three lead wires, can be installed in a 5 mm x 5 mm duct inside a rod 2.6 m long.

The space available in the duct is severely limited and has necessitated using very small diameter lead wires. A two wire, common dummy, installation was tried at first but gave problems with stability since the small lead wires were necessarily about four metres long. This was largely cured by changing to a three wire, common dummy situation, despite requiring even smaller lead wires.

3.   DATA COLLECTION

An automated data collection system was obviously essential in order to handle the large quantities of data that the tests would generate. The chosen system, which has been described in detail elsewhere [4, 5] consists of two units; a data logger and a supervising microcomputer.

The logger handles 208 input channels using constant current energisation which is switched to each channel in turn by reed-relay scanners.

The microcomputer controls the logger using purpose-written interfacing software and handles data storage on twin floppy disks. Software data transfer to a mainframe computer is also available which makes the power of a large machine available for subsequent data analysis.

4.   SPECIMEN DETAILS

The twelve specimens for the short-term tests were all 1500 mm long with cross-sections ranging from 70 x 70 mm up to 200 x 200 mm. They were reinforced with either 12 mm or 20 mm diameter strain gauged rods, positioned centrally. Both plain mild steel and ribbed high yield steel reinforcement was used. Details of the specimens are given in Table 1.

A number of different strain gauge layouts were tried with the early specimens but eventually a standard layout having 80 gauges each of 3 mm gauge length, spaced at 12.5 mm intervals along alternate halves of the central metre of each rod was adopted.

All specimens carried sets of Demec gauge points (200 mm gauge length) to allow measurement of average surface strains. Some specimens also contained embedment strain gauges (12 mm gauge length, overall size 30 mm x 9 mm x 2.5 mm). These were always restricted to one half of the specimens as it was considered that they might act as crack inducers. Depending on the specimen cross-section one, two or three rows of embedment gauges have been used to investigate the strain gradients from the reinforcing rod to the surface of the concrete.

Concrete for the specimens had a maximum aggregate size of 10 mm (determined by the spacing of the embedment gauges), a water:cement ratio of 0.6 and an aggregate:cement ratio of 5.5. Test cubes and cylinders were cast along with each specimen for determination of compressive strength and indirect tensile strength respectively.

Before concreting the rods were mounted in the test rig and load cycled in order to check fully the installation, and minimise any hysteresis. The results from this procedure were also used to calculate a Young's modulus value for each rod.

5.   TESTING EQUIPMENT AND PROCEDURES

The short-term tests were conducted in a purpose-built test rig and were each completed within one day. A manual hydraulic loading system was employed with the jack being located at the bottom of the specimen. Loading was measured by a flat load cell at the top of the specimen and displayed on a meter giving a direct digital read-out. The voltage output from the load cell was also connected directly into the data logger via an output from the meter.

The specimens were loaded incrementally with the increment sizes adjusted as the tests proceeded to reflect the rates at which changes were occurring within the specimen. In particular very detailed information was sought immediately before and after the formation of cracks and this often demanded load increments as fine as 0.5 kN.

The applied load and a full set of strain gauge readings were read and stored at every load stage. Time constraints precluded Demec readings being taken at all load stages, so a selective procedure was adopted with emphasis being given to the period during which the cracks formed. Crack widths were measured, when appropriate, at the same time as the Demecs, using an Ultra-Lomara 250 b microscope.

Loading of the specimens was halted when the reinforcement had fully yielded. With mild steel rods this often resulted in very high strain readings.

Cross-Section (mm x mm)	Bar Type & Dia (mm) R-Mild T-Torbar	% Reinforcement	Embedment Gauges Yes/No	Age At Test (days)	Cube Strength At Test (N/mm^2)	Indirect Tensile Strength At Test (N/mm^2)	No. of Cracks	Applied Load At First Crack (kN)	Reinforcement Strain At First Crack (microstrain)	Applied Load At Last Crack (kN)	Reinforcement Strain At Last Crack (microstrain)
70 x 70*	R12	1.80	No	28	45.5	3.1	5	12.0	134	15.5	161
70 x 70	R12	1.80	No	29	46.7	2.8	5	12.0	85	14.5	117
70 x 70	T12	1.80	No	28	47.3	3.0	8	12.5	120	18.5	177
100 x 100	R12	0.88	No	29	41.5	3.0	3	20.0	109	28.0	171
100 x 100	T12	0.88	Yes	29	45.0	2.7	4	18.0	98	30.0	162
100 x 100	R20	2.65	No	28	38.7	2.8	4	25.0	80	45.0	375
100 x 100	T20	2.65	Yes	28	46.7	3.1	7	12.5	52	40.0	281
140 x 140	T12	0.45	No	28	54.0	3.1	2	47.5	99	47.5	99
140 x 140	R20	1.35	No	29	42.0	3.1	2	47.5	165	55.0	223
140 x 140	T20	1.35	Yes	28	54.7	2.8	4	35.0	103	80.0	568
200 x 200	T20	0.66	Yes	28	60.3	3.1	1	65.0	83	-	-

* No gross yield of reinforcement

Table 1: Specimen Details and Test Results

Two tests had to be repeated. In the case of a 100 mm x 100 mm specimen having a 12 mm diameter high yield rod this was due to strain gauge stability problems and failure of the load measuring instrumentation during the test. It does not appear in Table 1. The 70 mm x 70 mm specimen having a 12 mm diameter mild steel rod was repeated because the expected gross yield of the reinforcement was not observed. Subsequent hardness measurements revealed that the rod was unusually hard, thus having an atypically high yield strength.

6.   RESULTS

Results for the short-term specimens are summarized in Table 1.

The cracks generally formed on the cast face of the specimens possibly due to the concrete being less completely compacted adjacent to the free surface and so having a lower Young's modulus. Once formed they usually extend around three faces of the specimen with compressive strains being recorded on the back face. Only occasionally would a crack propogate right round the specimen, and then usually only at high load levels.

More cracks formed in specimens reinforced with Torbar than in those reinforced with the plain mild steel rods, all other things being equal. Typical longitudinal strain distributions for R12 and T12 100 mm x 100 mm specimens are shown in Figures 1 and 2 and it can be seen that the changing strain profiles as the cracks developed have been clearly recorded.

Often quite considerable bending was recorded at the cracks, but away from the cracks the strain distributions were remarkably linear indicating near constant bond stresses along the specimens. These were higher in the case of the Torbar specimens, as would be expected.

It was common for peak reinforcement strains at the cracks to be higher than the rod strains outside the concrete, due to bending initiated by the cracking, and consequently gross yield in the mild steel rods always occured at a crack. There is some evidence to suggest that slipping between the reinforcement and the concrete, again at the cracks, was occurring with the mild steel rods but not with the Torbar. Debonding at the ends of the specimens was also observed when it extended into the strain-gauged section of the rods.

Reinforcement strains just prior to the formation of the final cracks could be surprisingly high (see Table 1), while in contrast there were strong indications that with specimens containing embedment gauges the first cracks formed at strains which were atypically low. With these specimens the first crack always formed in the region of an embedment gauge.

However, the embedment gauges have yielded useful information regarding strain profiles across the concrete and are giving an interesting indication of how load is shared between the reinforcement and the concrete particularly prior to cracking.

The above observations are based on an initial assessment of the large amount of numerical data generated by an investigation of this type. Much more detailed discussion will be possible when the data has been fully analysed using computer software which is currently being developed.

7.   CONCLUSIONS

The technique of internally strain gauging reinforcing rods has been developed to the stage where reliable detailed strain distributions can be obtained, even over long time periods.

The programme of tests already completed is enabling an improved understanding of tension stiffening and bond behaviour to be obtained for short-term loading
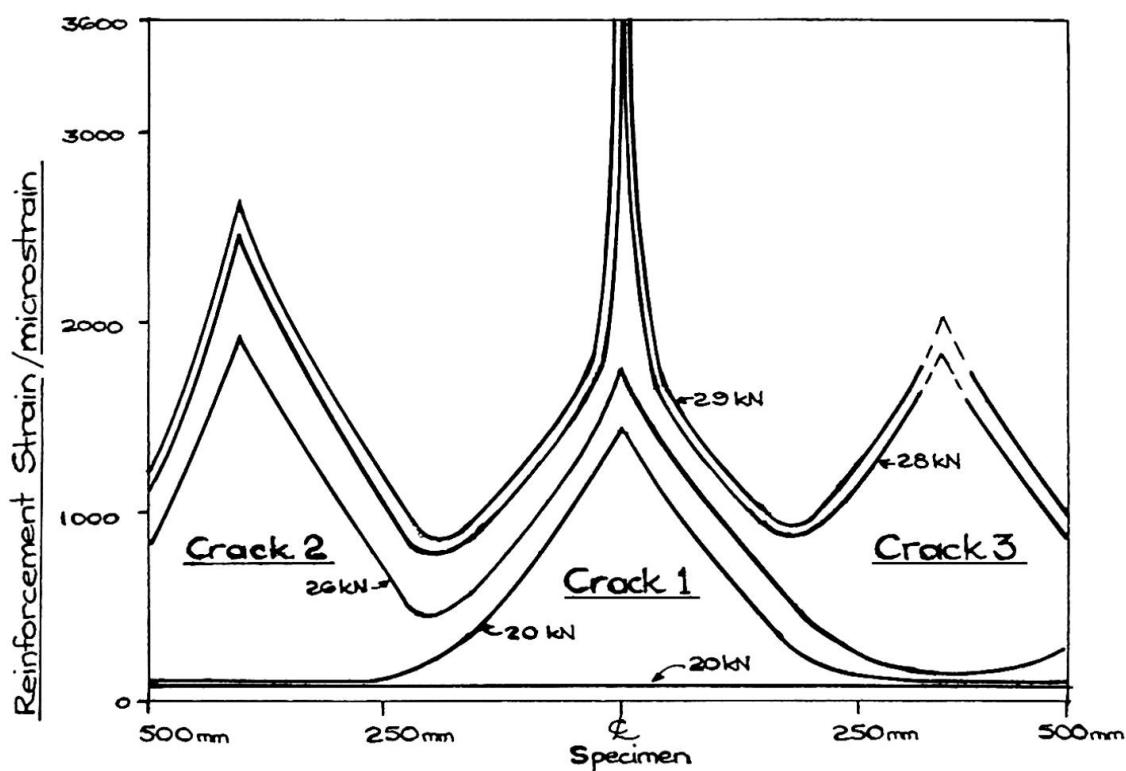
Fig 1 : STRAIN DISTRIBUTIONS FOR R12 100x100x1500 mm
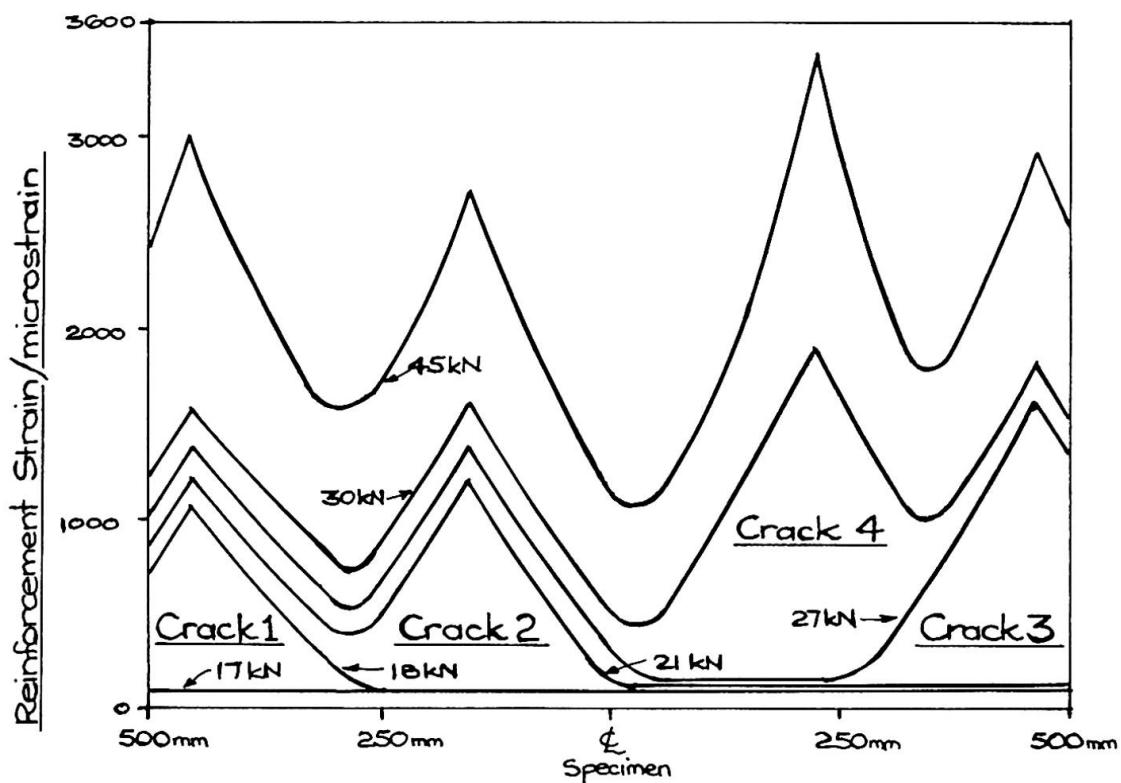
Fig 2 : STRAIN DISTRIBUTIONS FOR T12 100x100x1500 mm

conditions, and long-term tests are currently in progress which are enabling time-dependent effects to be studied.

Results to date are most encouraging and a full programme of analysis is currently being undertaken.

8.   ACKNOWLEDGEMENTS

9.   REFERENCES

1.   MAINS, R.M., "Measurement of the distribution of tensile and bond stresses along reinforcement bars". Journal of American Concrete Institute, Vol. 3, pp 225-252, 1951.

2.   NILSON, A.H., "Bond stress-slip relations in reinforced concrete". Report No. 345, Department of Structural Engineering, Cornell University, New York, 1971.

3.   SCOTT, R.H., and GILL, P.A.T., "Developments in the measurement of reinforcement strain distributions in reinforced concrete members". Strain, Vol. 18, pp 61-63, 1982.

4.   SCOTT, R.H., GILL, P.A.T., and MUNRO, M., "A modern data collection system and its interfacing requirements". Proceedings of Civil Comp 83, London, 1983.

5.   SCOTT, R.H., and GILL, P.A.T., "A modern data collection system". Strain, Vol. 20, pp 63-68, 1984.

Leere Seite

Blank page

Page vide

Design of Reinforced Concrete Structures against Impact and Impulsive Loading

Projet de structures en béton armé sous l'effet de chocs

Entwurf von Stahlbetonkonstruktionen unter Stossbelastung

Klaus BRANDES
Dr.-Ing.
Bundesanstalt für Materialprüfung
Berlin, BRD

Klaus Brandes, geboren 1936, promovierte an der Technischen Universität Berlin. Nach vier Jahren Tätigkeit an der TU Berlin ging er an die BAM. Dort ist er vor allem mit bautechnischen Sicherheitsvorkehrungen für Kernkraftwerke beschäftigt.

SUMMARY
Reinforced concrete structures are suited in a particular way to withstand impact and impulsive loading. In contrast to static loads there may be considerable excedance of the limits of elastic behaviour. In addition to the strain limitations, deformation limits for the design have to be defined and determined. Gaps in our knowledge concerning this field have become obvious in recent years. The subject of this paper is a survey on how to succeed in closing these gaps.

RESUME
Les structures en béton armé sont très appropriées pour reprendre des chocs de haute intensité. Par opposition aux sollicitations statiques, des déformations au-delà de la limite élastique sont possibles. En plus de la limitation des contraintes, il faut également prescrire des limites aux déformations. Ces derniers temps sont apparus des manques de connaissances évidents dans ce domaine que cette contribution essaye de combler.

ZUSAMMENFASSUNG
Stahlbetonkonstruktionen sind in besonderem Masse geeignet, Stoss- und Impulsbelastungen hoher Intensität zu widerstehen. Im Gegensatz zu statischen Beanspruchungen dürfen dabei die Grenzen elastischen Verhaltens erheblich überschritten werden. Zusätzlich zu Begrenzungen der Spannungen müssen auch Verformungsgrenzen für den Entwurf definiert und festgelegt werden. Kenntnislücken auf diesem Gebiet sind in letzter Zeit offensichtlich geworden. Über Bemühungen, die Lücken zu schliessen und deren Erfolge wird kurz berichtet.

1. INTRODUCTION

Definitions in standards for the design of reinforced concrete structural members against impact and impulsive loading with high intensity differ from definitions established for static loads in such a way that besides the stress limits also limits for deformations have to be stated. This is still a rather new field and knowledge herein is imcomplete. Only in the past years relevant investigations - experimental and theoretical-numerical - have been performed; their results being the basis for an initial approach to set up rules. Further investigations are still necessary, especially experimental ones, to generalize the so far attained findings and place them on a broad basis.

2. PROBLEM DESCRIPTION

Reinforced concrete structures are well suited to withstand impact and impulsive loads of high intensity. They have a large mass and may reach, by an appropriate constructive design, large plastic deformations. The fact that the ability to strongly deform under short-term loading is essential, may be clarified by comparison of a simple reinforced concrete beam under static and short-term loading. With static loading, the deformation in the elastic range increases proportional with the load (fig. 1). When yielding starts in the cross-section, the deformation increases overproportional and after reaching the maximum value R_u of the force-deformation-curve (limit load), a point has been reached beyond with statical allowable conditions become impossible.
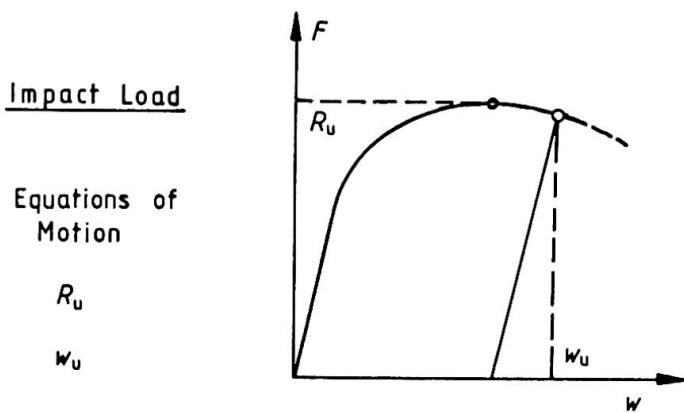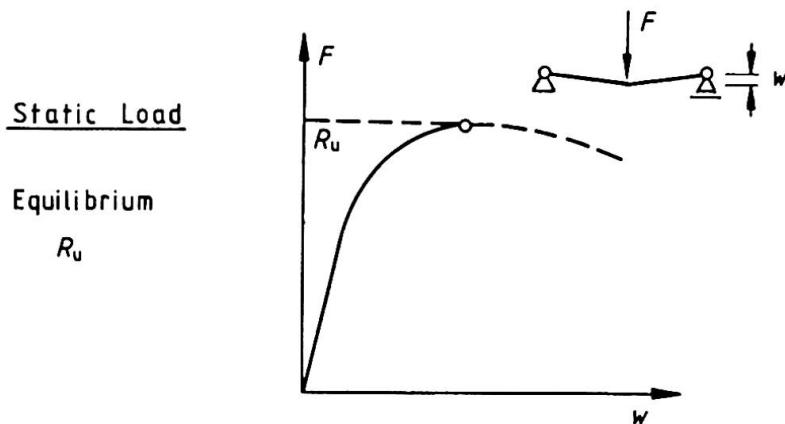

Fig. 1
Simply supported beam under static and under impact load. Load-deflection-diagram and characteristic values.

However, impact loads may exceed the value R_u (fig. 2). The structural member then follows the equations of motion.

The portion of the applying load F exceeding the value $R = R(w)$ causes an accelerated deformation, mainly in the plastic range. Inertia forces, however, counteract this movement.

The plastic deformation is completed, if the impact force F drops below the actual value of R. To analyse the behaviour of the beam it is necessary that the curve $R(w)$, and for a design formulation the value w_u (fig. 1) is known.

The solution of these problems is complicated insomuch as yield stress and tensile strength depend on the strain rate (fig. 3). Some results of the investigation confirm a similar dependence of the fracture deformation /1/.
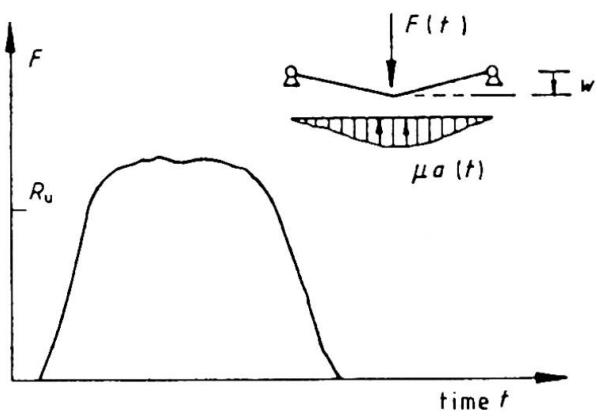
Fig. 2
Impact loaded beam.
Impact force-time diagram, simple one-degree-of-freedom-system and resistance-deflection-curve.
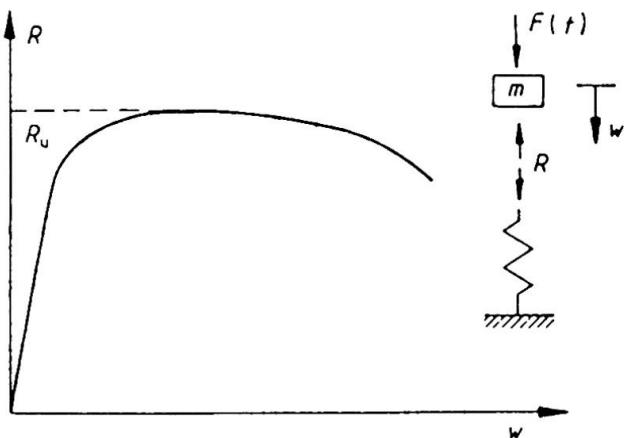
3. INVESTIGATIONS, RESULTS, DEFINITONS

In the past years, extensive investigations, regarding a solution of these problems, were performed in the Federal Republic of Germany, also in Great Britain, France, Switzerland, the Netherlands and some other countries. A RILEM-symposium in 1982 also treated this topic in detail /2/.
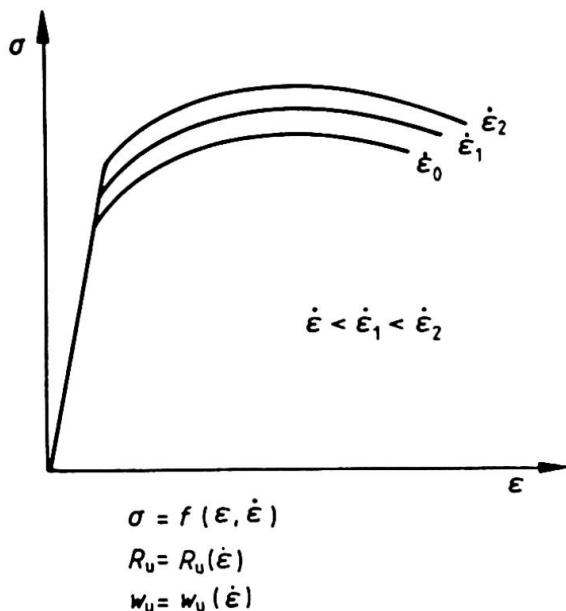
Fig. 3
Strain rate effect
on reinforcing
steel, schematical
representation /6/

$$\sigma = f(\varepsilon, \dot{\varepsilon})$$
$$R_u = R_u(\dot{\varepsilon})$$
$$w_u = w_u(\dot{\varepsilon})$$

For impulsive loading and stresses due "soft missile impact", re-
quirements on strain and deformation limits in plastic hinges
can now be established, because of recent investigations. In the
german nuclear code draft KTA 2203 /3/, the strain in the rein-
forcement, have been limited to 0.8-times that of the uniform
elongation in tension tests (1.6 % ... 2.5 %). Regarding the
rotational capacity θ_p of a yield hinge, the value from ACI
349-76 /4/,

$$\theta_p = 0.0065 \frac{d}{x} \leq 0.07$$

was assumed for the limitation of rotation in plastic hinges,
still requiring a re-examination. A survey on so far existing
definitions is given in fig. 4.

The dependence of the material strength on the strain rate has
been reflected in factors only by ACI 349-76. Investigations at
the Federal Institute for Material Testing (BAM) confirm these
statements /6/, fig. 5.

The safety assessment still has not been solved with stating
these requirements, because safety factors were introduced for
both stress limits and deformation limits whose coupling depends
upon the overall system under consideration /7/.

4. SCOPE

First steps have been made to determine and define the proper-
ties of reinforced concrete structural members under impact and
impulsive loading necessary for the engineer to design a struc-
ture. Further investigations, especially tests, are required to
close the still existing gaps in knowledge. One question would,
for example, concern the validity range of the meanwhile deter-
mined mathematical interrelationships describing the dependence
of material characteristic values on the strain rate, but also
the question regarding the influence of the strain rate history
/6/.

Reinforced Concrete Structural Members /

Reinforcing Steel

U L T I M A T E   D E F O R M A T I O N

Design Values / Observed Values

CEB_Model_Code (8.3): Plastic Rotation (static load):

$$\vartheta_{p,u} = \begin{cases} 0.007 & \text{for } x/d = 0.6 \\ \vdots \\ 0.040 & \text{for } x/d = 0.1 \end{cases}$$

ACI_349-76: Plastic Rotation (static and dynamic load):

$$\vartheta_{p,u} = 0.0065 \ d/x \leqq 0.07$$

KTA_2203 (draft 1983): Plastic Rotation:

$$(\vartheta_{p,u} = 0.0065 \ d/x \leqq 0.07)$$

Uniform plastic strain in reinforcement:

$$\varepsilon_{d,u}^{p} = 0.8 \ A_g \leqq 2.5 \ \% \ ^*)$$

Observed_Values   (BAM - Investigation):

$$\vartheta_{p,obs,u} = \begin{cases} 0.19 & (\text{dyn.load, } f_y = 420 \text{ MPA}) \\ \vdots \\ 0.08 & (\text{stat.load, } f_y = 1100 \text{ MPa}) \end{cases}$$

$^*)$ A_g uniform plastic elongation in tension test

Fig. 4 Requirements for deformation of plastic hinges or strain in reinforcemnet bars. Comparison of design values in several codes with observed values

$f_{y,o}$	$f_{y,imp}/f_{y,o}$	
N/mm^2	ACI 349-76	BAM-Investig.
280	120 %	
350	115 %	
420	110 %	111 %
1100	100 %	100 %

Fig. 5   Strain rate dependent strength of
reinforcing steel

REFERENCES

/1/ LIMBERGER, E., BRANDES, K., and HERTER, J.
Influence of Mechanical Properties of Reinforcing Steel on
the Ductibility of Reinforced Concrete Beam with Respect
to High Strain Rates. /2/, Proceedings, pp. 134-145.

/2/ RILEM-CEB-IABSE-IASS-Interassociation Symposium
Concrete Structures under Impact and Impulsive Loading.
Berlin, June 2-4, 1982. Introductory Report (1982),
Proceedings (1982), Final Report (1983)

/3/ KTA 2203. Schutz von Kernkraftwerken gegen Flugzeugabsturz.
Auslegung der baulichen Anlagen (bei vorgegebenen Lastan-
nahmen). Entwurf, Dezember 1983.

/4/ ACI 349-76. Code Requirements für Nuclear Safety Related
Concrete Structures. ACI-Journal, Feb. 1977

/5/ CEB-FIP Model Code for concrete structures. Bulletin
d'information CEB No. 124-125 / 1978

/6/ BRANDES, K. und LIMBERGER, E., Zur Beeinflussung der Festig-
keitskennwerte von Betonstahl durch die Dehngeschwindigkeit
Beton- und Stahlbetonbau 1984

/7/ BRANDES, K., Behaviour of Critical Regions of RC-Structures
under Soft Missile Impact and Impulsive Loading. /2/,
Introductory Report, 1982

Conclusions to Seminar IX
Developments in the Design of Reinforced and Prestressed Concrete Structures

Renaud FAVRE
Professor
Swiss Fed. Inst. of Technology
Lausanne, Switzerland

Five papers were presented orally at this session by Messrs. M. Fukuhara, Japan; R. Favre, Switzerland; J. Schlaich, Federal Republic of Germany; G. Causse, France; and R. Green, Canada. The session had a good success with 200 participants. The call for papers based on Mr. Wicke's general report had provoked 46 responses which had to be reduced to 8 contributions for the Final Report. The design of reinforced concrete and prestressed concrete structures remain among the most attractive topics.

It is clear that concrete structures, with their enormous economic impact, with sophisticated methods of construction, with time-dependent effects such as creep and shrinkage, give rise to a lot of interesting problems. In recent years, the public was especially confronted with the serviceability, the durability and aesthetical aspects. Engineers have the bad feeling that a considerable part of their analysis is useless and does not help to design the desired good and economic structure, and that many important aspects are not considered in the analysis because of lack of knowledge.

This session has contributed to fill some gaps. Detailing, one of the most important parts in the design process, has generally been treated in a subjective way. A consistent design of reinforced concrete structures, as already developed by the author within CEB, has been presented. Use of concrete columns in tall buildings, associated with big earthquake loads, needs shear reinforcement which can be realized with stirrups made of high resistance steel. The long term behaviour of columns has a big impact in the case of second order problems. Also in the usual case of braced columns in a building, normally with a moderate slenderness ratio, one has to take into account the long-term behaviour for the serviceability limit state. It has been shown how a design procedure, based on a verification of the section resistance of a column under the combined action of a normal force N and a bending moment M, should advantageously be replaced by a procedure based on N and imposed angle deformations at both ends of the column.

Finally, the excellent behaviour of model test scale 1 : 1 of a bridge girder with spatial truss similar to the Bubiyan bridge construction in Kuwait was presented.

Leere Seite

Blank page

Page vide